Physics of Fluids ARTICLE pubs.aip.org/aip/pof

Hyper-reflection of inertia-gravity waves by vortices

Cite as: Phys. Fluids **38**, 054102 (2026); doi: 10.1063/5.0330610
Submitted: 21 February 2026 · Accepted: 15 April 2026 ·
Published Online: 1 May 2026

View Online Export Citation CrossMark

C. Nolan and E. S. Benilov[a)]

AFFILIATIONS

Department of Mathematics and Statistics, University of Limerick, Limerick V94 T9PX, Ireland

[a)]Author to whom correspondence should be addressed: Eugene.Benilov@ul.ie. URL: https://eugene.benilov.com/

ABSTRACT

We examine scattering of waves by a vortex under the *f*-plane approximation. Two kinds of vortices are considered: eddies (where the angular velocity decreases monotonically with radius) and rings (where the angular velocity peaks at a certain radius before decaying). Both kinds can reflect more energy than the incident wave carries, but over-reflection by eddies is relatively weak, whereas that by rings can be infinitely strong (hyper-reflection). The difference is attributed to stronger or weaker centrifugal force and other curvature-related effects. It is also shown that a hyper-reflecting flow is always marginal to a range of unstable flows, but the converse does not hold: flows that are unstable at frequencies lower than the minimum frequency of inertia-gravity waves cannot radiate; hence, do not hyper-reflect. Finally, we derive an asymptotic model for the coupled dynamics of a vortex and a spectrum of small-amplitude random waves. It is shown that, if the vortex hyper-reflects a certain wavenumber and this wavenumber is present in the spectrum, hyper-reflection almost immediately drains a significant proportion of the vortex's energy.

I. INTRODUCTION

It is well known that jets can over-reflect waves, so that the energy of the scattered field exceeds that of the incident wave.[1–14] The excess energy is transferred from the flow to the wave through their interaction at the critical level, i.e., the straight line where the streamwise component of the wave's phase speed matches the local velocity of the fluid particles. Over-reflection has also been shown to exist for vortices,[15,16] in which case the critical level is a circle where the azimuthal component of the wave's velocity matches the fluid velocity. Over-reflection of waves by vortices can also be caused by circles where the radial component of the wave's phase speed vanishes;[17–19] this type of over-reflection is akin to the so-called super-radiance of black holes.[20]

It is natural to assume that a mechanism transferring energy from a jet or a vortex to waves is likely to cause instability of the former, with the latter playing the role of unstable perturbations. This has indeed been shown to occur for various kinds of waves and various geometries of the reflecting flows.[6,21–37] Note that this kind of instability (often called "radiative") is relatively slow, so that the unstable jet or vortex survives for a long time in a metastable state.

The present paper examines the limiting case of over-reflection, where the energy of the scattered field is infinite. This effect is often referred to as "resonant over-reflection," but we shall use the rarer but shorter term "hyper-reflection." So far, hyper-reflection (H-R) has been observed only for jets;[4,38–41] as argued in Ref. 41, H-R occurs when the incident wave experiences multiple reflections within the vortex and is amplified each time it passes through a critical level (for more details, see Sec. III A 3). It has also been argued that this effect is responsible for bursts of energy observed numerically at a large distance from the jet by Viúdez and Dritschel.[42] More generally, H-R is important for wave-flow energy exchange in atmospheres and oceans of planets.

In the present paper, we demonstrate that vortices also hyper-reflect, but only within a relatively narrow range of parameters. As a result, this effect is much harder to detect than hyper-reflection by jets. Nevertheless, we have found numerous examples of hyper-reflecting vortices, but only for rings (where the angular velocity peaks at a certain radius, then decays) and never for eddies (where the angular velocity monotonically decays toward infinity). Interestingly, both eddies and rings support neutrally stable oscillations typically associated with H-R,[41] but those in eddies are always sub-inertial, i.e., their frequency is lower than the minimum frequency of inertia-gravity waves. As a result, they cannot be radiated into the open ocean, whereas neutral oscillations in rings can be superinertial, hence, give rise to H-R.

This paper has the following structure. In Sec. II, we formulate the problem mathematically. In Secs. III A and III B, we present our theoretical and numerical results, respectively. In Sec. IV, we discuss the relationship of hyper-reflection with radiative instability, as H-R waves are, in essence, neutrally stable radiative modes. In Sec. V, we explore how waves affect the vortex scattering them.

II. FORMULATION

A. Governing equations and the vortex solution

Consider a sphere rotating with an angular velocity Ω and let a thin layer of an ideal fluid adhere to its surface due to gravity. If one is interested in the flow dynamics near a certain reference point of the sphere, one can take advantage of the f-plane approximation,[43] i.e., replace the spherical surface with a tangent plane, rotating about an axis normal to itself, with the frequency $f = 2\Omega \sin\phi$, where ϕ is the latitude of the reference point. We shall also use the shallow-water approximation.

Our interest in vortices suggests the use of polar coordinates, i.e., the radius r and azimuthal angle θ. We also introduce the time t, the acceleration due to gravity g, the fluid's depth h, the radial velocity u, and the azimuthal velocity v.

Under the f-plane and shallow-water approximations, the flow is governed by the following equations:[43]

$$\frac{\partial u}{\partial t} + u\frac{\partial u}{\partial r} + \frac{v}{r}\left(\frac{\partial u}{\partial \theta} - v\right) + g\frac{\partial h}{\partial r} = fv, \tag{1}$$

$$\frac{\partial v}{\partial t} + u\frac{\partial v}{\partial r} + \frac{v}{r}\left(\frac{\partial v}{\partial \theta} + u\right) + \frac{g}{r}\frac{\partial h}{\partial \theta} = -fu, \tag{2}$$

$$r\frac{\partial h}{\partial t} + \frac{\partial (ruh)}{\partial r} + \frac{\partial (vh)}{\partial \theta} = 0. \tag{3}$$

These equations also describe a two-layer fluid if one of the layers is much thinner than the other and g is the reduced gravity (i.e., the regular gravity multiplied by the relative density difference between the layers). Such an approximation—sometimes called a "1.5-layer model"—applies to both the ocean and the atmosphere (in the former, the upper "active" layer is much thinner than the lower "passive" layer, whereas in the latter the opposite is true).

Let h_0 be a characteristic value of the depth, using which one can define the so-called internal Rossby radius $L = \sqrt{gh_0}/f$ and introduce the following nondimensional variables:

$$r_{nd} = \frac{r}{L}, \quad \theta_{nd} = \theta, \quad t_{nd} = tf,$$
$$h_{nd} = \frac{h}{h_0}, \quad u_{nd} = \frac{u}{Lf}, \quad v_{nd} = \frac{v}{Lf}.$$

Rewriting Eqs. (1)–(3) in terms of the nondimensional variables and omitting the subscript $_{nd}$, we obtain

$$\frac{\partial u}{\partial t} + u\frac{\partial u}{\partial r} + \frac{v}{r}\left(\frac{\partial u}{\partial \theta} - v\right) + \frac{\partial h}{\partial r} = v, \tag{4}$$

$$\frac{\partial v}{\partial t} + u\frac{\partial v}{\partial r} + \frac{v}{r}\left(\frac{\partial v}{\partial \theta} + u\right) + \frac{1}{r}\frac{\partial h}{\partial \theta} = -u, \tag{5}$$

$$r\frac{\partial h}{\partial t} + \frac{\partial (ruh)}{\partial r} + \frac{\partial (vh)}{\partial \theta} = 0. \tag{6}$$

Equations (4)–(6) admit a steady solution, describing a radially symmetric vortex,

$$h = H(r), \quad u = 0, \quad v = V(r),$$

where H and V satisfy the so-called gradient-wind balance,[44]

$$\frac{\mathrm{d}H}{\mathrm{d}r} - V - \frac{1}{r}V^2 = 0. \tag{7}$$

Physically, this condition reflects the balance of the pressure gradient, Coriolis force, and centrifugal force [the first, second, and third terms in equality (7), respectively].

In what follows, it is assumed that

$$H \to 1, \quad V \to 0 \quad \text{as} \quad r \to \infty, \tag{8}$$

where the first limit implies an appropriate choice of the scale h_0 used for nondimensionalization.

Finally, we shall need the energy conservation law, which can be deduced by considering the following combination of the governing equations:

$$rhu \times (1) + rhv \times (2) + \left(\frac{u^2}{2} + \frac{v^2}{2} + h\right) \times (3),$$

and thus obtain

$$r\frac{\partial E}{\partial t} + \frac{\partial Q_r}{\partial r} + \frac{\partial Q_r}{\partial \theta} = 0, \tag{9}$$

where

$$E = \frac{h(u^2 + v^2) + h^2}{2}$$

is the planar density of energy and

$$Q_r = ruh\left(\frac{u^2 + v^2}{2} + h\right), \quad Q_\theta = vh\left(\frac{u^2 + v^2}{2} + h\right)$$

are the components of the energy flux.

B. Linearization and harmonic solutions

Scattering of waves by vortices is described by solutions of the form,

$$u = \varepsilon\tilde{u}(t, r, \theta) + \mathcal{O}(\varepsilon^2), \quad v = V(r) + \varepsilon\tilde{v}(t, r, \theta) + \mathcal{O}(\varepsilon^2),$$
$$h = H(r) + \varepsilon\tilde{h}(t, r, \theta) + \mathcal{O}(\varepsilon^2),$$

where the tilded variables describe the wave and ε is a small parameter characterizing the wave amplitude. Linearizing equations (4)–(6), one obtains

$$\frac{\partial \tilde{u}}{\partial t} + \frac{V}{r}\left(\frac{\partial \tilde{u}}{\partial \theta} - \tilde{v}\right) - \frac{\tilde{v}}{r}V + \frac{\partial \tilde{h}}{\partial r} = \tilde{v}, \tag{10}$$

$$\frac{\partial \tilde{v}}{\partial t} + \tilde{u}\frac{\mathrm{d}V}{\mathrm{d}r} + \frac{V}{r}\left(\frac{\partial \tilde{v}}{\partial \theta} + \tilde{u}\right) + \frac{1}{r}\frac{\partial \tilde{h}}{\partial \theta} = -\tilde{u}, \tag{11}$$

$$r\frac{\partial \tilde{h}}{\partial t} + \frac{\partial (r\tilde{u}H)}{\partial r} + \frac{\partial \left(V\tilde{h} + \tilde{v}H\right)}{\partial \theta} = 0. \tag{12}$$

Given the linearity of the problem, it is sufficient to examine harmonic solutions,

$$\tilde{u} = 2\mathrm{Re}\,[\hat{u}(r)e^{\mathrm{i}(k\theta-\omega t)}], \tag{13}$$

$$\tilde{v} = 2\mathrm{Re}\,[\hat{v}(r)e^{\mathrm{i}(k\theta-\omega t)}], \tag{14}$$

$$\tilde{h} = 2\mathrm{Re}\,[\hat{h}(r)e^{\mathrm{i}(k\theta-\omega t)}]. \tag{15}$$

Without loss of generality, ω can be assumed positive, whereas k can be either positive or negative, but necessarily an integer [otherwise solution (13)–(15) is not be periodic in θ]. The direction of the wave propagation is determined by the sign of the phase speed ω/k—hence, by that of k.

Substitution Eqs. (13)–(15) implies that we consider a single wave focused on the center of the vortex, which is an idealized situation, rarely arising in the real ocean. It is examined only as a first step, just to elucidate the qualitative properties of wave scattering by vortices. With this done, the results will be extended to a broad spectrum of waves propagating in all directions (see Sec. V).

Substituting Eqs. (13)–(15) into Eqs. (10)–(12), one obtains

$$\mathrm{i}\left(\frac{kV}{r}-\omega\right)\hat{u} - \left(1+\frac{2V}{r}\right)\hat{v} + \frac{\mathrm{d}\hat{h}}{\mathrm{d}r} = 0, \tag{16}$$

$$\mathrm{i}\left(\frac{kV}{r}-\omega\right)\hat{v} + \left(1+\frac{V}{r}+\frac{\mathrm{d}V}{\mathrm{d}r}\right)\hat{u} + \frac{\mathrm{i}k}{r}\hat{h} = 0, \tag{17}$$

$$\mathrm{i}\left(\frac{kV}{r}-\omega\right)\hat{h} + \frac{1}{r}\frac{\mathrm{d}(r\hat{u}H)}{\mathrm{d}r} + \frac{\mathrm{i}kH}{r}\hat{v} = 0. \tag{18}$$

Equations (16) and (17) can be used to express $\hat{u}$ and $\hat{v}$ through $\hat{h}$,

$$\hat{u} = \mathrm{i}F\frac{-\left(1+\frac{2V}{r}\right)\frac{k}{r}\hat{h} + \left(\omega-\frac{kV}{r}\right)\frac{\mathrm{d}\hat{h}}{\mathrm{d}r}}{H}, \tag{19}$$

$$\hat{v} = F\frac{-\left(\omega-\frac{kV}{r}\right)\frac{k}{r}\hat{h} + \left(1+\frac{V}{r}+\frac{\mathrm{d}V}{\mathrm{d}r}\right)\frac{\mathrm{d}\hat{h}}{\mathrm{d}r}}{H}, \tag{20}$$

where

$$F = \frac{H}{\left(1+\frac{V}{r}+\frac{\mathrm{d}V}{\mathrm{d}r}\right)\left(1+\frac{2V}{r}\right) - \left(\omega-\frac{kV}{r}\right)^2}. \tag{21}$$

Substituting expressions (19) and (20) into Eq. (18), one obtains, after straightforward algebra,

$$\frac{\mathrm{d}}{\mathrm{d}r}\left(rF\frac{\mathrm{d}\hat{h}}{\mathrm{d}r}\right) - \left\{\frac{k^2}{r}F + \frac{k\frac{\mathrm{d}}{\mathrm{d}r}\left[\left(1+\frac{2V}{r}\right)F\right]}{\omega-\frac{kV}{r}} + r\right\}\hat{h} = 0. \tag{22}$$

This equation has arisen in numerous papers, mainly in the context of the stability of vortices (e.g., Refs. 45–47).

Equation (22) requires boundary conditions for $\hat{h}$ at $r = 0$ and as $r \to \infty$, which are discussed in Sec. II C.

C. Boundary conditions

Equation (22) describes an arbitrary linear perturbation superposed on a vortex. To single out a free wave coming from infinity and reflecting back, one needs to examine the behavior of $\hat{h}(r)$ as $r \to \infty$.

Under boundary conditions (8), Eqs. (21) and (22) reduce to a particular case of the Bessel equation,

$$\frac{\mathrm{d}}{\mathrm{d}r}\left(\frac{r}{1-\omega^2}\frac{\mathrm{d}\hat{h}}{\mathrm{d}r}\right) - r\hat{h} = 0 \quad \text{as} \quad r \to \infty. \tag{23}$$

Either recalling the asymptotics of the Bessel functions or carrying out basic asymptotic analysis of Eq. (23), one can deduce that

$$\hat{h} = r^{-1/2}\left(C_- e^{-\mathrm{i}qr} + C_+ e^{\mathrm{i}qr}\right) + \mathcal{O}(r^{-3/2}) \quad \text{as} \quad r \to \infty, \tag{24}$$

where $C_\pm$ are the arbitrary constants and

$$q = \sqrt{\omega^2 - 1} \tag{25}$$

is, physically, the radial wavenumber. In what follows, q will be used to characterize the wave instead of ω, with the latter given by $\omega = \sqrt{1+q^2}$ (which is the nondimensional dispersion relation of inertia-gravity waves).

Substituting asymptotics (24) into solution (13), one can see that $e^{-\mathrm{i}qr}$ describes a wave propagating toward the center of the vortex, whereas $e^{\mathrm{i}qr}$ describes the wave propagating toward infinity. Thus, to describe scattering, we set $C_- = 1$ (the incident wave has unit amplitude) and $C_+ = R$ (where R is the reflection coefficient), and obtain

$$\hat{h} = r^{-1/2}(e^{-\mathrm{i}qr} + Re^{\mathrm{i}qr}) + \mathcal{O}(r^{-3/2}) \quad \text{as} \quad r \to \infty. \tag{26}$$

One also needs a boundary condition at the center of the vortex. To derive it, note that, as $r \to 0$, one of the two linearly independent solutions of Eq. (22) tends to zero ($\hat{h} \sim r^{|k|}$) and the other, to infinity ($\hat{h} \sim r^{-|k|}$). In most problems—such as vortex stability, for example—one would routinely discard the latter. In the problem at hand, however, the singular solution is physically meaningful: it describes a circular wave focusing onto, or defocussing away from, the origin.

This issue is examined in Appendix A. It turns out that, in the end, the condition of regularity does apply, which amounts to

$$\hat{h} = \mathcal{O}(r^{|k|}) \quad \text{as} \quad r \to 0. \tag{27}$$

This condition implies that the singularities of the focusing/incoming and defocussing/outgoing waves cancel each other. Physically, their superposition can be viewed as a standing mode with a node at $r = 0$.

Boundary-value problem (22), (26) and (27) determines both $\hat{h}(r)$ and R. Situations where $|R| > 1$ will be referred to as over-reflection of the wave (k, q) by the vortex with a profile $H(r)$.

III. RESULTS

A. Analytical results

1. The unitarity condition

As shown in Ref. 41, the scattering coefficients for jets satisfy a certain "unitarity condition," and a similar condition holds for vortices. Since the coefficients of Eq. (22) are real, the complex conjugate of the solution is also a solution, hence, the Wronskian of $\hat{h}$ and $\hat{h}^*$, which can be defined as

$$Wr = \mathrm{i}rF\left(\frac{\mathrm{d}\hat{h}}{\mathrm{d}r}\hat{h}^* - \frac{\mathrm{d}\hat{h}^*}{\mathrm{d}r}\hat{h}\right), \tag{28}$$

does not depend on r. Then, recalling asymptotics (27) as $r \to 0$ and asymptotics (26) as $r \to \infty$, one can show that

$$\lim_{r\to 0} Wr = 0, \qquad \lim_{r\to\infty} Wr = \frac{2}{q}\left(|R|^2 - 1\right). \tag{29}$$

These two results and the constancy of Wr imply that $|R| = 1$, so that no over-reflection occurs.

Note, however, that the Wronskian theorem holds only for equations with smooth coefficients, but if they are singular at some points, the Wronskian can "jump," i.e., abruptly change its value. This circumstance is important, as the coefficients of Eq. (22) are indeed singular at critical levels, i.e., the points r_c such that

$$\frac{\omega}{k} = \frac{V}{r} \quad \text{at} \quad r = r_c, \tag{30}$$

and also points r_a such that

$$\left(1 + \frac{V}{r} + \frac{\mathrm{d}V}{\mathrm{d}r}\right)\left(1 + \frac{2V}{r}\right) = \left(\omega - \frac{kV}{r}\right)^2 \quad \text{at} \quad r = r_a, \tag{31}$$

in which case the coefficient F becomes singular [see Eq. (21)]. For reasons explained later, these singularities will be referred to as "apparent."

2. Critical levels

Physically, equality (30) makes the azimuthal component of the wave's phase speed match the angular velocity of the vortex. Similar singularities (but with the linear phase speed and velocity) arise in jets. It is well known that over-reflection never occurs in a jet without critical levels, and the same will be shown for vortices in this subsection.

Critical levels—both in jets and generally—can be regularized by expanding the model: consider arbitrary-evolving disturbances instead of harmonic ones,[48–51] or nonlinear disturbances,[52,53] or include in the model dissipation.[54] Then the new effect should be phased out: the limiting solution would behave singularly on both sides of the critical level, but the two behaviors would be inter-related in a physically meaningful way.

In this work, critical levels are regularized by dissipation. As shown by Case[48] and Dikiy[49] for a similar problem, the limiting behavior of the solution does not depend on the nature of dissipation, allowing one to use the simplest option—the so-called Rayleigh viscosity—i.e., replace ω with $\omega + \mathrm{i}\varepsilon$ and take the limit $\varepsilon \to 0^+$. In the context of the problem at hand, the Rayleigh viscosity is justified physically: it would arise naturally if Eqs. (1)–(3) were modified to describe weak viscous friction between the flow and the ocean's bottom[43] (in which case ε would be the friction coefficient).

Thus, replace $\omega \to \omega + \mathrm{i}\varepsilon$ in Eqs. (21) and (22) and introduce a local variable, $\xi = r - r_c$. A Frobenius-style analysis yields two linearly independent solutions of the form,

$$\begin{gathered}\hat{h}_1 = \xi + \mathcal{O}(\xi^2),\\ \hat{h}_2 = 1 - B_c\xi[\ln(\xi - \beta_c\mathrm{i}\varepsilon) - 1] + \mathcal{O}(\xi^2\ln\xi) \quad \text{as} \quad \xi \to 0,\end{gathered} \tag{32}$$

where

$$B_c = \left\{\frac{\dfrac{\mathrm{d}}{\mathrm{d}r}\left[\left(1 + \dfrac{2V}{r}\right)F\right]}{rF\dfrac{\mathrm{d}}{\mathrm{d}r}\left(\dfrac{V}{r}\right)}\right\}_{r=r_c}, \qquad \beta_c = \operatorname{sgn}\left[k\frac{\mathrm{d}}{\mathrm{d}r}\left(\frac{V}{r}\right)\right]_{r=r_c}. \tag{33}$$

For $\varepsilon > 0$, both $\hat{h}_1$ and $\hat{h}_2$ are analytic at the critical level, but in the limit $\varepsilon \to 0$, only $\hat{h}_1$ is analytic, whereas $\hat{h}_2$ is such that

$$\begin{gathered}\hat{h}_2 = 1 - B_c\xi(\ln|\xi| - 1 - \beta_c\mathrm{i}\pi) + \mathcal{O}(\xi^2\ln\xi) \quad \text{as} \quad \xi \to 0^-,\\ \hat{h}_2 = 1 - B_c\xi(\ln|\xi| - 1) + \mathcal{O}(\xi^2\ln\xi) \quad \text{as} \quad \xi \to 0^+.\end{gathered}$$

Let the general solution be

$$\hat{h} = A_1\hat{h}_1 + A_2\hat{h}_2, \tag{34}$$

where $A_{1,2}$ are the arbitrary constants. Then, calculating Wronskian (28) and keeping in mind that $\hat{h}(0) = A_2$ [as follow from Eqs. (34) and (32)], one obtains

$$\lim_{\varepsilon\to 0}\left(\lim_{\xi\to 0^+} Wr - \lim_{\xi\to 0^-} Wr\right) = 2\beta_c\pi B_c|\hat{h}(0)|^2. \tag{35}$$

Assume for simplicity that there is only one critical level. Then, the constancy of the Wronskian within the intervals $(0, r_c)$ and (r_c, ∞) and equalities (29), Eqs. (34) and (35) yield

$$|R|^2 = 1 + \pi q\left\{\frac{\dfrac{\mathrm{d}}{\mathrm{d}r}\left[\left(1 + \dfrac{2V}{r}\right)F\right]}{\left|\dfrac{\mathrm{d}}{\mathrm{d}r}\left(\dfrac{V}{r}\right)\right|\operatorname{sgn} k}|\hat{h}|^2\right\}_{r=r_c}. \tag{36}$$

Identity (36) allows one to test a given vortex and a given wave for over-reflection: one should find the position of the critical level and check the sign of the expression in the curly brackets on the right-hand side of Eq. (36). If this expression is positive, the critical level over-reflects (amplifies the wave), and it under-reflects (dampens the wave) otherwise.

Identity Eq. (36) can also be used to distinguish over-reflecting and non-over-reflecting vortices.

To do so, select an arbitrary point in the vortex's profile. Denoting the wavenumbers of the wave that has a critical level at this point by (k, q) and taking into account that

$$\omega = \frac{kV(r_c)}{r_c}, \qquad \operatorname{sgn} k = \operatorname{sgn} V(r_c),$$

one can examine the sign of the expression in the curly brackets in identity (36) and thus verify that a vortex over-reflects if and only if

$$V\frac{\mathrm{d}}{\mathrm{d}r}\left(\frac{H}{1 + \dfrac{V}{r} + \dfrac{\mathrm{d}V}{\mathrm{d}r}}\right) > 0. \tag{37}$$

All examples of $H(r)$ which we examined while working on this problem happen to satisfy this criterion at least for some r, and we have been unable to find an example for which (37) is never satisfied. Even though this does not prove that all vortices over-reflect, this is a good indication that they do.

Finally, identity (36) can be readily extended to situations with several critical levels. Denoting their total number by N and treating the subscript $_c$ as the critical level's number, one obtains

$$|R|^2 = 1 + \pi q\sum_{c=1}^{N}\left\{\frac{\dfrac{\mathrm{d}}{\mathrm{d}r}\left[\left(1 + \dfrac{2V}{r}\right)F\right]}{\left|\dfrac{\mathrm{d}}{\mathrm{d}r}\left(\dfrac{V}{r}\right)\right|\operatorname{sgn} k}|\hat{h}|^2\right\}_{r=r_c}.$$

3. Apparent singularities

Despite the singularity of the coefficient F at points determined by condition (31), the solution of Eq. (22) is such that Wronskian (28) is continuous. For jets, this has been shown by Boyd,[55] and for vortices, in Appendix B of the present paper.

Since apparent singularities do not affect the continuity of the Wronskian, one might conjecture that they can be completely removed from Eq. (22) by a suitable substitution, the same way they were removed from a similar problem by Vanneste and Yavneh[56] and Wang and Balmforth.[57] Such a conjecture is further supported by the fact that the singular terms in the Frobenius expansion of $\hat{h}$ near an apparent singularity cancel beyond the order necessary for continuity of W (see the Appendix B).

Physically, apparent singularities seem to be important. As argued in Ref. 41, they typically flank an over-reflecting critical level on both sides, acting as potential barriers, and the resulting multiple reflections give rise to a resonance causing H-R. Note that the presence of two apparent singularities is a necessary, but not a sufficient condition for H-R, as two barriers form a resonator only if they are separated by a certain distance. Furthermore, the barriers created by apparent singularities are partially transparent and, thus, let the captured waves "leak" from the resonator. This circumstance imposes an extra requirement: H-R can occur only if the energy lost through leakage is small enough to be replenished when the waves pass through the over-reflecting critical level.

B. Numerical results

It turns out that the strength of over-reflection by a vortex depends on whether its angular velocity, V/r, is a monotonic function of r. For the sake of brevity, we shall refer to monotonic vortices as eddies and to non-monotonic as rings (because these can be viewed as circular, ring-like currents). Some examples of eddies and rings can be found in Fig. 1.

The difference between the two kinds of vortices will be illustrated using the following example:

$$H = 1 + \Delta H \frac{\tanh\dfrac{r_v - r}{W} + \tanh\dfrac{r_v + r}{W}}{2\tanh\dfrac{r_v}{W}}, \tag{38}$$

where ΔH, W, and r_v are the vortex's amplitude, width, and radius, respectively. Straightforward algebra shows that profile (38) with

$$\frac{r_v}{W} < \ln\left(5 - 2\sqrt{6}\right)^{-\frac{1}{2}} \approx 1.1462,$$

represents eddies, and it represents rings otherwise. Note also that, in the limit

$$r_v/W \to \infty,$$

profile (38) tends to the so-called Bickley jet (tested for over- and hyper-reflection by Refs. 39 and 41, respectively). We have also tested examples other than (38)—inter alia, with erf instead of arctan —and found that (38) is qualitatively representative of all vortices.

When choosing parameters for illustrating our results, we kept in mind that quasigeostrophic vortices (such that $|\Delta H| \ll 1$) are characterized by small angular velocity and allow for critical levels only for waves with large k [see equality (30)]. It has turned out, however, that over-reflection of such waves is weak and so this parameter range is of little interest. Thus, we shall focus on strongly ageostrophic vortices and illustrate our results using the particular case $\Delta H = \pm 0.9$. Physically, this parameter range describes oceanic near-surface lenses and similar large-amplitude vortices.

Boundary-value problem (22), Eqs. (26) and (27) was solved numerically using the algorithm described in Appendix C. The results obtained are described below.

1. Eddies

It has turned out that over-reflection of waves by anticyclonic eddies is weak. For the eddy shown in dotted line in Fig. 1, for example, $|R| \lesssim 1.00001$ for all (k, q). One might think that over-reflection would strengthen for smaller W—i.e., larger shear of the vortex flow—but the gradient-wind balance (7) with a large negative $\mathrm{d}H/\mathrm{d}r$ makes V complex. Physically, this means that the hydrostatic pressure gradient and centrifugal force are too strong to be balanced by the Coriolis force.

For cyclonic eddies ($\Delta H < 0$), no such problem arises, as the centrifugal force acts against the pressure gradient and with the Coriolis force, so that the limit $W \to 0$ does not make V complex. It turns out, however, that, with decreasing W, $|R|$ grows very slowly: even for $W = r_v = 0.05$ (and $\Delta H = -0.9$), the maximum value of $|R|$ is less than 1.02. Given that W is nondimensionalized by the Rossby radius, we conclude that over-reflection by sensibly sized cyclonic eddies is insignificant.

2. Rings

The scattering properties of rings depend primarily on r_v (i.e., the ratio of its dimensional radius to the Rossby radius).

Unsurprisingly, rings with sufficiently small radii behave similarly to eddies. For $r_v = 2$ and $\Delta H = 0.9$, for example, hyper-reflection (H-R) does not occur for any W, and even over-reflection is weak: $|R| \lesssim 1.04$ for all W and (k, q).

The scattering properties of larger rings are different: if r_v exceeds a certain threshold (for $\Delta H = 0.9$, it is between 2.7 and 2.8), there exists a value of W for which H-R occurs for a certain range of k (see Figs. 2 and 3).

The following comments are in order:

- Hyper-reflected waves correspond to first-order poles of the reflection coefficient, which was established by computing the function $|R(q - q_h)|$, where q_h is the radial wavenumber of the H-R wave, and showing that

$$L = \lim_{q \to q_h} |R(q - q_h)| < \infty.$$

This result is illustrated in the lower panels of Figs. 2 and 3.

- Interestingly, the actual values of the limit L happen to be rather small; in the cases illustrated in Figs. 2 and 3, for example, $L \lesssim 0.04$. As a result, the H-R peaks appear narrow: if q moves away from q_h by, say, 0.1, the reflection coefficient $|R|$ becomes order-one.
- The H-R peaks are also sensitive to small changes of W. If, for example, curve $k = -4$ in Fig. 2 were redrawn for $W = 0.6500$

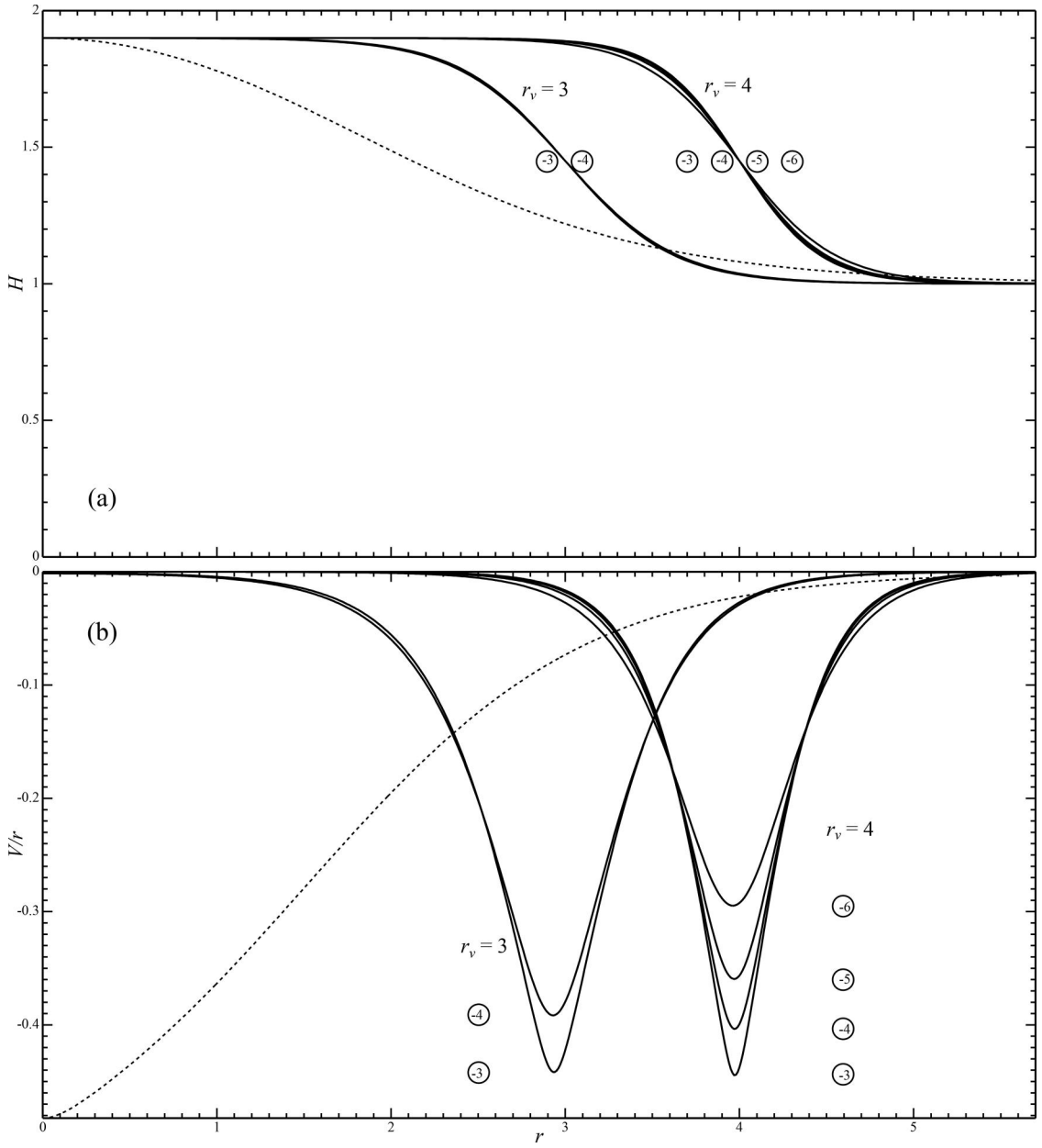

FIG. 1. Examples of rings described by expression (38): (a) depth, (b) angular velocity. Rings with $\Delta H = 0.9$ are shown in solid line: the two rings with $r_v = 3$ correspond to $W \approx 0.6149, 0.6370$; and the four rings with $r_v = 4$ correspond to $W \approx 0.4571, 0.4690, 0.4904, 0.5437$. The circled numbers show the azimuthal wavenumber k at which the rings hyper-reflect (their scattering characteristics are illustrated in Figs. 2 and 3). The dotted line shows an eddy with $r_v = W = 1.74$ (does not hyper-reflect).

(instead of $W = 0.6370$), the maximum reflection coefficient would be $|R| \approx 1.11$ (instead of $|R| \approx \infty$).

The high sensitivity of H-R to parameter changes likely stems from its resonant nature, i.e., even a small variation of, say, the width W can tune the ring out of resonance. This should affect observability of H-R in the real ocean. One should keep in mind, however, that real vortices are influenced by large-scale flows and changing oceanic conditions, and thus evolve continuously. If, during this evolution, the vortex happens to hyper-reflect, it would almost instantly lose an order-one fraction of its energy (more details given later is Sec. V).

- As r_v increases, the range of k where H-R\occurs expands: for $r_v = 3$, it is $k = -3, -4$; for $r_v = 4$, it is $k = -3, -4, -5, -6$, etc.
- H-R also occurs for cyclonic rings, but for larger q and smaller W. For $r_v = 3$, $\Delta H = -0.9$, and $k = 4$, for example, H-R occurs at $q \approx 2.128$ and $W \approx 0.1037$, whereas the anticyclonic

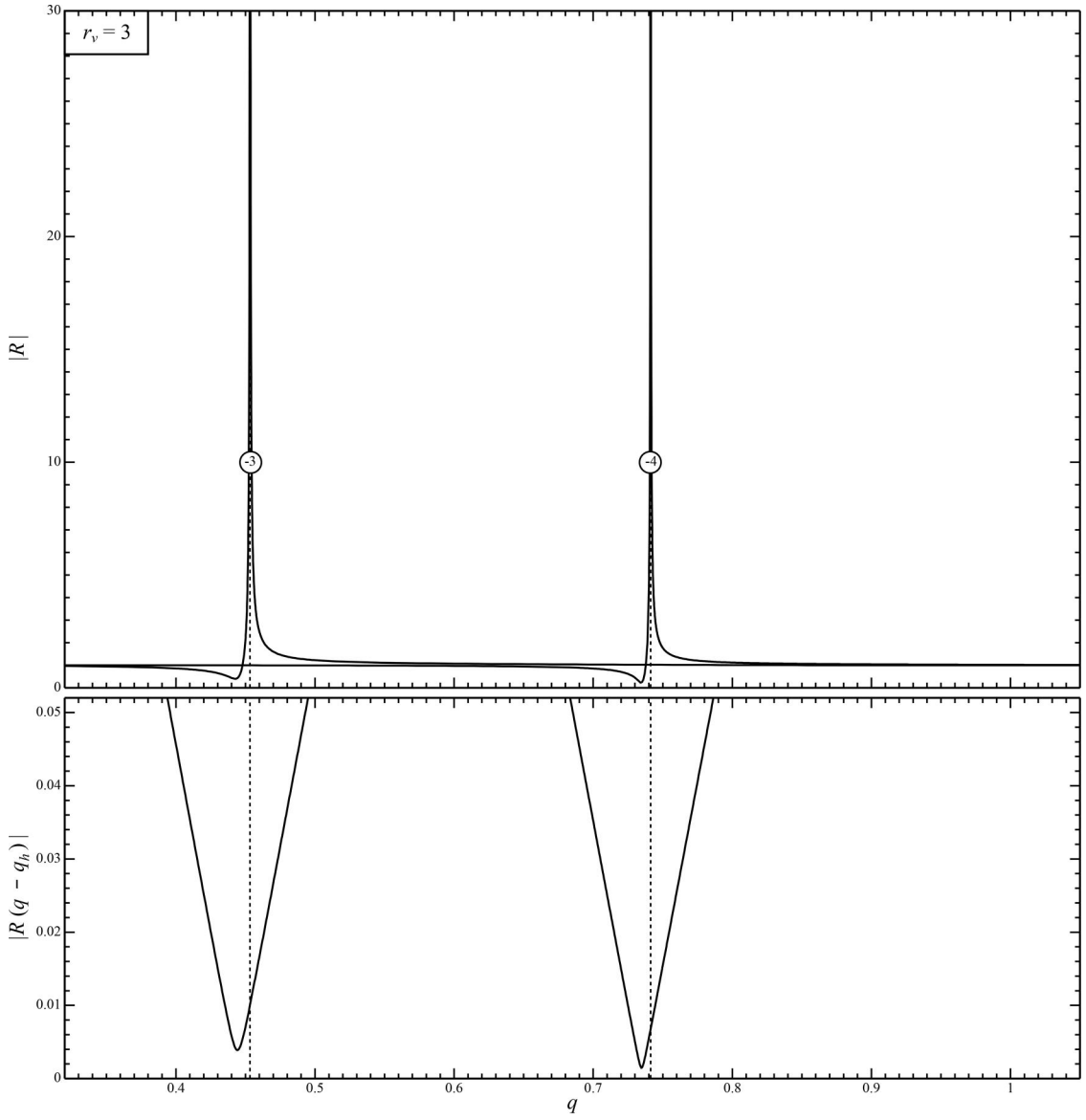

FIG. 2. Dependence of the reflection coefficient on the radial wavenumber, for rings (38) with $\Delta H = 0.9$ and $r_v = 3$. The two curves correspond to $W \approx 0.6149$ (hyper-reflects waves with $k = -3$) and $W \approx 0.6370$ (hyper-reflects waves with $k = -4$). For $k \geq -2$, critical levels do not exist (hence, $|R| = 1$ for all W and q); for $k \leq -5$, critical levels exist but do not cause hyper-reflection ($|R| \lesssim 1.066$ for all W and q). The wavenumbers q_h of the hyper-reflected waves are marked with dotted lines. The lower panel illustrates that the H-R singularity is a first-order pole, $|R| \sim |q - q_h|^{-1}$.

counterpart of this ring over-reflects at $q \approx 0.7413$ and $W \approx 0.6370$.

- Recall that critical levels can be either over- or under-reflecting (depending on whether or not condition (37) is satisfied). With this in mind, it is interesting to interpret H-R in terms of the locations of the available critical levels and apparent singularities.

  We found that H-R always occurs when the over-reflecting critical level is located between two apparent singularities, whereas the other critical level can be either over- or under-reflecting (see Fig. 4). The same pattern has previously been noted for jets in Ref. 41.
- More generally, Ref. 41 hypothesized that H-R occurs when a wave "oscillates to and fro between two apparent singularities acting as barriers, and each time it passes through the over-reflecting critical level, its amplitude grows." It should be emphasized that the barriers created by the apparent singularities are partially transparent, but the energy leaking through them is replenished when the wave passes through the over-reflecting critical level.

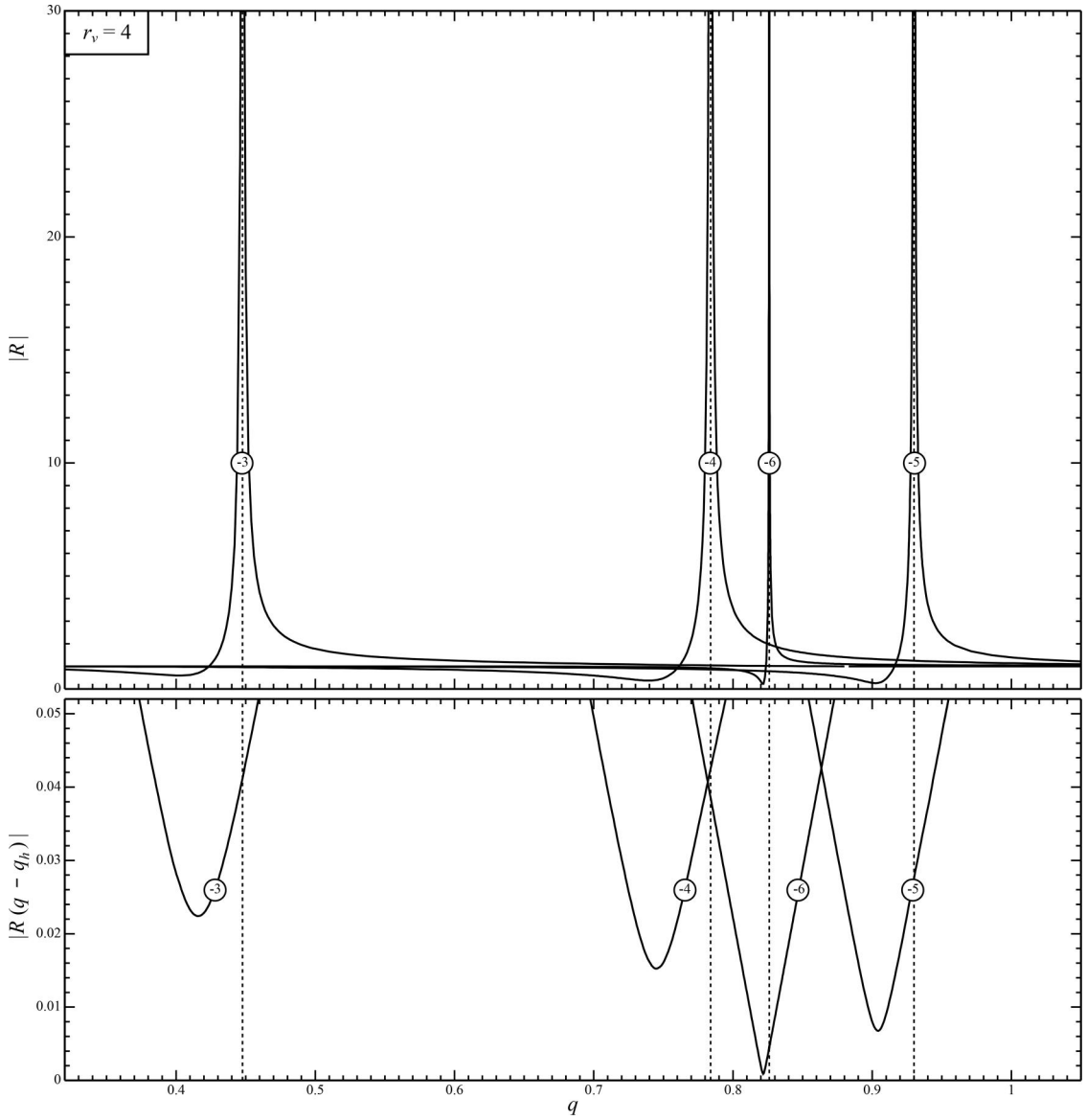

FIG. 3. As in Fig. 2, but for rings with $\Delta H = 0.9$, $r_v = 4$, and $W \approx 0.4571,\ 0.4690,\ 0.4904,\ 0.5437$ (hyper-reflect waves with $k = -3, -4, -5, -6$, respectively).

The same happens for vortices, as the over-reflecting critical level is always located between two apparent singularities (as illustrated in Fig. 4).

- According to Ref. 41, the Bickley jet hyper-reflects for all values of the parameters involved, whereas its vortex counterpart, ring (38), hyper-reflect only if its width W assumes one of several discrete values.

  To understand why, recall that, for a ring, the azimuthal wavenumber k of the hyper-reflected wave must be an integer, whereas for a jet, the corresponding parameter (stream-wise wavenumber) does not have to. Thus, the extra requirement in the former case implies an extra constraint on the ring's parameters.
- Intuitively, one should expect that hyper-reflected waves should always exist in the large wave number limit,

$$k \to \infty, \qquad q \to \infty,$$

but only if the wave's azimuthal velocity remains finite, and that critical levels exist,

$$\frac{q}{|k|} \to \text{const} < \max\left|\frac{V}{r}\right|.$$

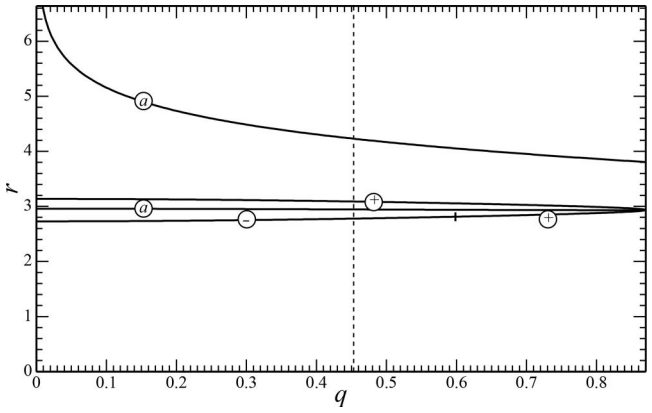

FIG. 4. Positions of the singular points vs q, for the waves with $k = -3$ and the ring with $\Delta H = 0.9$, $r_v = 3$, and $W \approx 0.6149$ (these parameter values correspond to curve −3 in Fig. 2). Circled *a* marks the apparent singularities, circled + and − mark the over- and under-reflecting critical levels, respectively. The point where one of the critical level switches from under- to over-reflection is marked on the corresponding curve with a vertical tick. The wavenumber of hyper-reflection is marked with a dotted line (observe that H-R occurs when one of the critical levels under-reflects).

IV. DISCUSSION

A. Hyper-reflection and radiative instability

To examine a vortex for radiative instability, one can reemploy two of the three tools used for hyper-reflection: linearized equation (22) and boundary condition (27) at the center of the vortex. Boundary condition (24) at infinity, in turn, should be modified by setting $C_- = 0$ and, thus, omitting the incident wave. Letting also $C_+ = 1$ (which does not cause loss of generality due to the linearity of the problem), one obtains

$$\hat{h} = r^{-1/2} e^{iqr} + \mathcal{O}(r^{-3/2}) \quad \text{as} \quad r \to \infty. \tag{39}$$

Equation (22) and conditions (27) and (39) form an eigenvalue problem where $\hat{h}(r)$ is the eigenfunction and ω the eigenvalue. The vortex is stable if all existing eigenvalues are such that $\mathrm{Im}\ \omega \le 0$.

Recall that the radial wavenumber q is related to ω by dispersion relation (25); hence, q is generally complex. Keeping in mind that the eigenfunction should not grow as $r \to \infty$ and the radiated wave travels away from the vortex, one should complement boundary condition (39) with

$$\mathrm{Im}\, q \ge 0, \qquad \mathrm{Re}\, q \ge 0.$$

Dispersion relation (25) shows that these conditions can be both satisfied only if $\mathrm{Im}\, \omega \ge 0$, i.e., for unstable or neutrally stable disturbances. In the latter case, $\mathrm{Im}\, q = 0$, and condition (39) describes a cylindrically diverging wave without an incident one, i.e., hyper-reflection.

This conclusion does not come as a surprise: as shown in Ref. 41 for jets, a hyper-reflected wave is always marginal to a range of unstable disturbances captured by the jet; thus, either an increase or a decrease in any parameter renders the wave unstable and spatially localized. We have checked (but did not include the actual derivation in the present paper) that a similar conclusion applies to vortices: an infinitesimal change of the ring's width W or amplitude ΔH, or radius r_v turns a hyper-reflected wave into an unstable disturbance decaying as $r \to \infty$.

To confirm and illustrate this conclusion, the instability problem for rings was solved numerically by shooting. Two branches (modes) of unstable disturbances have been found. For both, the dependence of ω on W (with ΔH and r_v fixed) and that of ω on ΔH (with W and r_v fixed) are illustrated in the left- and right-hand parts of Fig. 5, respectively. Note that the values of the fixed parameters, $W = 0.637$ and $\Delta H = 0.9$, were chosen to correspond to a hyper-reflected wave with $k = -4$.

Evidently, both modes are unstable in finite intervals of W and ΔH, bordered by two pairs of disturbances with $\mathrm{Im}\, \omega = 0$, but only one of these four is an H-R wave.

To understand why, observe that the other three neutrally stable disturbances are sub-inertial ($\omega < 1$), i.e., outside the frequency range of free inertia-gravity waves, for which $\omega = \sqrt{1 + q^2} \ge 1$. We conclude that sub-inertial disturbances cannot propagate away from, and are captured by, the vortex.

We conclude that the radiative and non-radiative/captured instabilities occur in the transparent and opaque parts of the wave spectrum, respectively.

The corresponding eigenfunctions are illustrated in Fig. 6: an example of a radiative disturbance is shown in panel (a) and two examples of non-radiative disturbances are shown in panels (b) and (c). Observe that the amplitude of the radiated wave in panel (a) is decreasing with distance, and not only due to cylindrical divergence, but also because its radial wavenumber q has a positive imaginary part (unlike that of a hyper-reflected wave).

Thus, hyper-reflection always indicates that the corresponding ring becomes unstable if its parameters are slightly changed. Yet this does not make H-R uninteresting or unimportant, as unstable geophysical vortices do not necessarily disintegrate. They are associated with "blobs" differing from the surrounding fluid by physical characteristics (temperature, salinity, density, etc.). Unlike unstable vortices in homogeneous media, such a blob can disintegrate only if it breaks up into smaller blobs; otherwise, it radiates waves and slowly spins down while spreading out and becoming thinner. The former scenario occurs only for large geophysical vortices,[58–61] whereas smaller ones should keep radiating for a long time. It is no coincidence that the characteristic times of radiative instability are typically small (see, for example, Refs. 6, 21–34, and 36 and the lower panels of Fig. 5 of the present paper).

B. Jets vs rings vs eddies

Consider a parallel flow on the f-plane, characterized by the depth profile $H(y)$ where y is the cross-stream coordinate, and the velocity profile is

$$U = \frac{\mathrm{d}H}{\mathrm{d}y}.$$

Let this flow be a unidirectional jet, i.e.,

$$U(y) > 0,$$
$$U \to 0 \quad \text{as} \quad y \to \pm\infty,$$

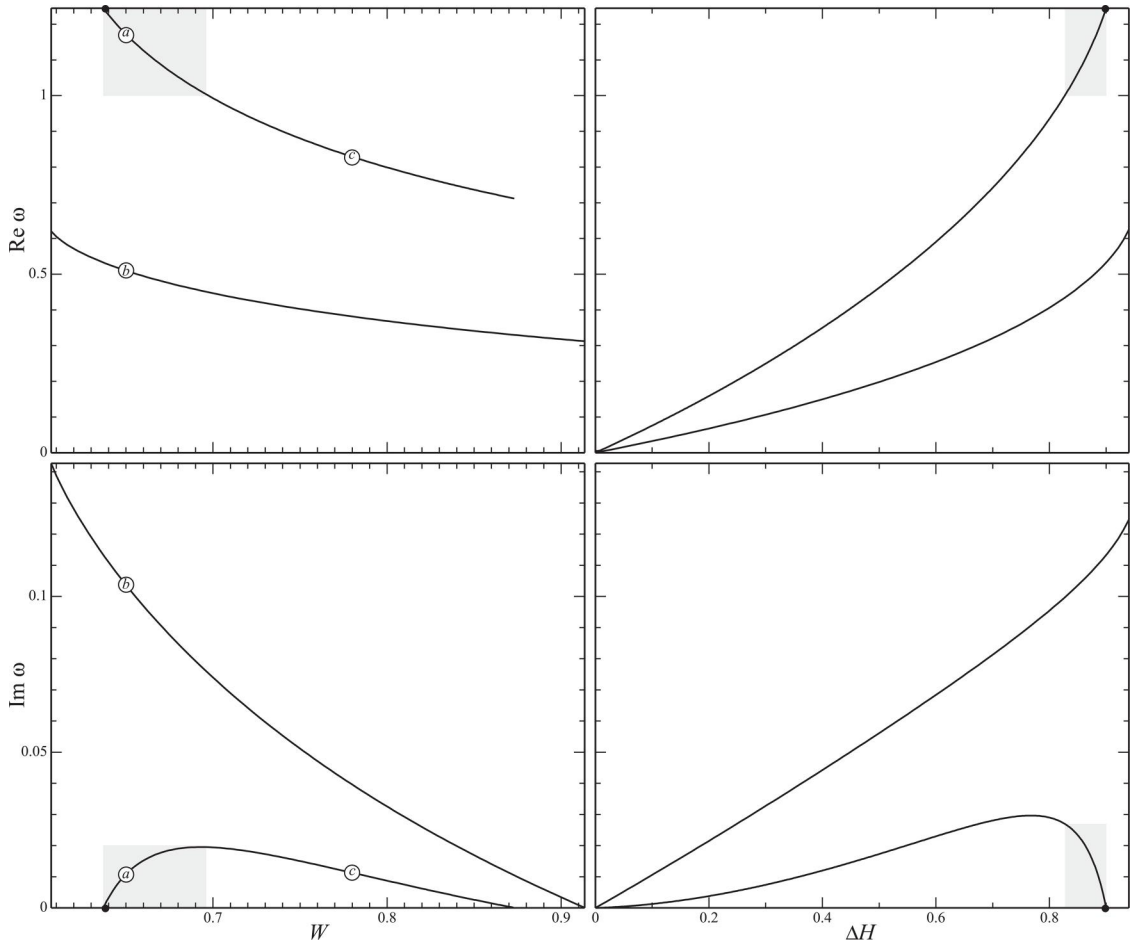

FIG. 5. The frequency ω of disturbances with $k = -4$ for rings described by expression (38) with $r_v = 3$. The left-hand panels show the graph of ω vs W, for $\Delta H = 0.9$; the right-hand panels show ω vs ΔH, for $W = 0.637$. The regions of radiative instability ($\mathrm{Re}\omega > 1$) are shaded, the black dots mark the hyper-reflected wave (it corresponds to the peak labeled "−4" in Fig. 2). The eigenfunctions corresponding to the points *a*, *b*, and *c* are plotted in Figs. 6(a)–6(c), respectively.

and introduce the nondimensional potential vorticity (PV),

$$Q = \left(1 - \frac{\mathrm{d}U}{\mathrm{d}y}\right)\frac{1}{H}.$$

It can be readily shown that, at the jet's maximum, $\mathrm{d}Q/\mathrm{d}y$ is positive, but it becomes negative as $y \to \pm\infty$. Thus, the PV gradient changes its sign, making all jets on the *f*-plane potentially unstable, and all of the particular examples examined so far have indeed turned out to be (e.g., Refs. 62 and 63 and references therein).

Recalling that instability and hyper-reflection are related, one can further conjecture that all jets hyper-reflect as well, and the particular examples examined in Ref. 41 agree with this hypothesis.

Thus, the present results and those of Ref. 41 can be summarized as follows:

- All jets are likely to hyper-reflect.
- A large ring hyper-reflects only if its width assumes a value from a certain set.
- Eddies and small rings never hyper-reflect.

The three kinds of flows can also be characterized by the extent to which they are affected by shear and centrifugal force (the latter depends on the flow's curvature):

- Jets are affected only by shear.
- Large rings are affected by shear and, to some extent, centrifugal force and other curvature-related effects.
- Small rings and eddies are affected by centrifugal force and curvature more strongly than the other two kinds of flows.

A comparison of the two sets of bullets suggests that centrifugal force and curvature weaken over-reflection and, if sufficiently strong, stop hyper-reflection.

Thus, the scattering properties of a ring and a jet are close only if the ring's width is smaller than its radius of curvature, and the centrifugal force is weaker than the Coriolis force. Nondimensionally, these conditions amount to

$$\frac{W}{r_v} \ll 1, \qquad \frac{1}{r_v W} \ll 1,$$

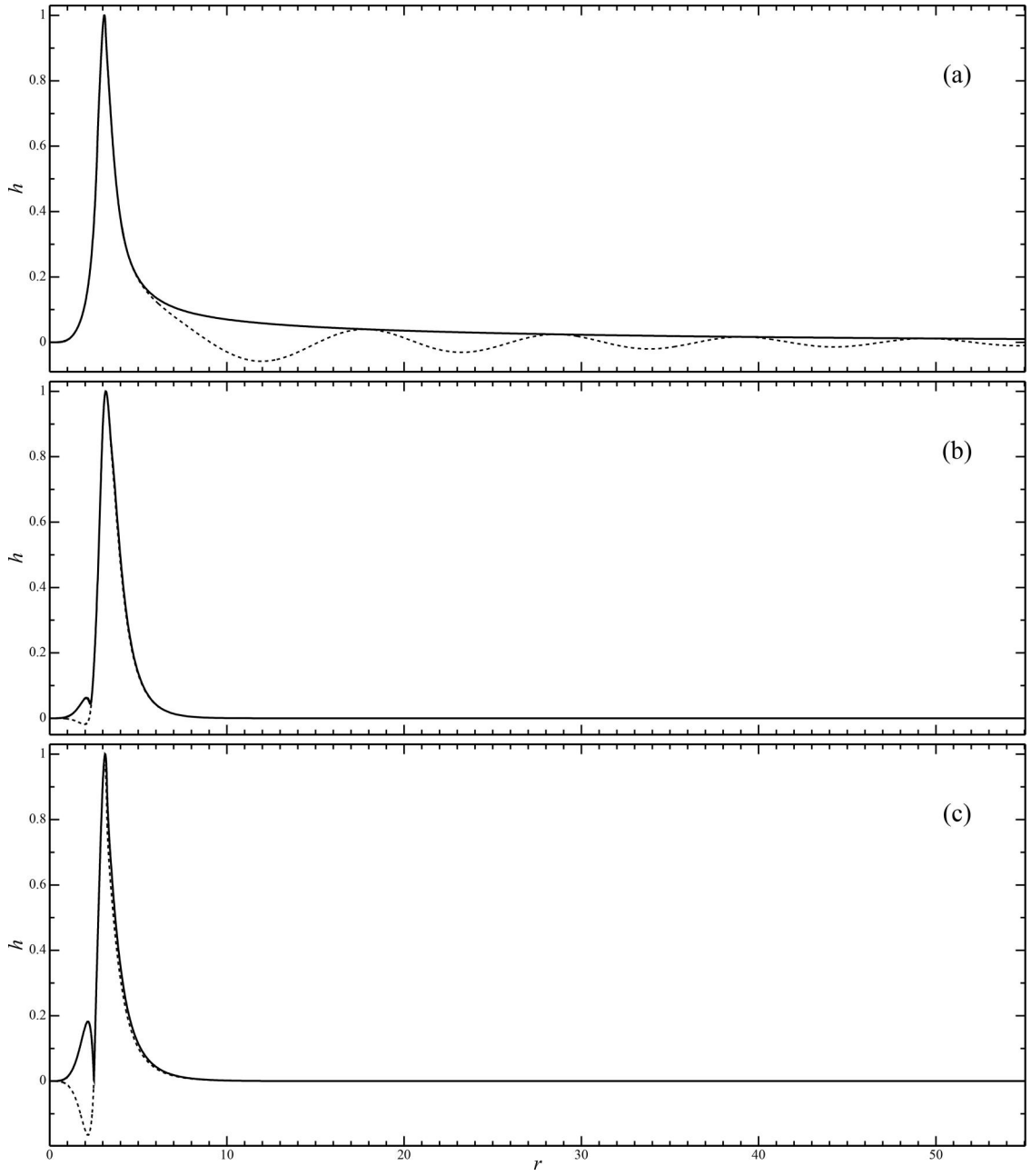

FIG. 6. Unstable disturbances with $k = -4$ for rings described by expression (38) with $r_v = 3$ and $\Delta H = 0.9$. The solid and dotted curves show $|\hat{h}|$ and $\mathrm{Re}\hat{h}$, respectively. The panel labels correspond to the points marked by circled *a*, *b*, and *c* in Fig. 5: (a) and (b) show the radiative and non-radiative disturbances for $W = 0.65$; (c) shows one of the two non-radiative disturbances for $W = 0.85$.

respectively. Note also that, for the hyper-reflecting rings illustrated in Figs. 2 and 3,

$$\max\left\{\frac{W}{r_v}\right\} \approx 0.2, \qquad \max\left\{\frac{1}{r_v W}\right\} \approx 0.5.$$

These numbers illustrate how far a ring can be from a jet and still hyper-reflect.

Note that, in the limit $r_v \to \infty$, the rings' curvature becomes small and their scattering properties should tend to those of jets. This is indeed the case: numerical experiments show that rings with large r_v hyper-reflect more waves, and the radial wavenumbers of these waves are more densely distributed. This effect can be observed even for moderate values of r_v—compare Fig. 2 ($r_v = 3$) and Fig. 3 ($r_v = 4$).

V. HOW DO THE WAVES AFFECT THE VORTEX?

The mere fact that the amplitude of a wave reflected by a vortex is infinite suggests a strong impact of the former on the latter. More generally, over-/under-reflected waves weaken/strengthen the vortex, respectively, and it is unclear whether a wide spectrum of inertia-gravity waves (which is always present in the real ocean—see, for example, Ref. 64 and references therein) drains or pumps up oceanic vortices. A similar problem was examined by Benilov *et al.*[65] for Rossby waves and straight flows.

A. Dynamics of the vortex

Let ε be a measure of the wave amplitude. It is clear (and agrees with the results of Ref. 65) that the vortex evolves at a timescale $\sim \varepsilon^{-2}$, so that the asymptotic method of multiple scales should be useful in this problem. Introducing, thus, the slow time,

$$T = \varepsilon^2 t,$$

and treating it as an independent variable alongside t, we rewrite the governing equations (4)–(6) in the form

$$\frac{\partial u}{\partial t} + \varepsilon^2 \frac{\partial u}{\partial T} + u\frac{\partial u}{\partial r} + \frac{v}{r}\left(\frac{\partial u}{\partial \theta} - v\right) + \frac{\partial h}{\partial r} = v, \tag{40}$$

$$\frac{\partial v}{\partial t} + \varepsilon^2 \frac{\partial v}{\partial T} + u\frac{\partial v}{\partial r} + \frac{v}{r}\left(\frac{\partial v}{\partial \theta} + u\right) + \frac{1}{r}\frac{\partial h}{\partial \theta} = -u, \tag{41}$$

$$r\frac{\partial h}{\partial t} + \varepsilon^2 \frac{\partial h}{\partial T} + \frac{\partial (ruh)}{\partial r} + \frac{\partial (vh)}{\partial \theta} = 0, \tag{42}$$

and expand the solution in ε up to the second order,

$$\begin{aligned} u &= \varepsilon\tilde{u}(t,r,\theta) + \varepsilon^2\tilde{u}_2(t,r,\theta) + \mathcal{O}(\varepsilon^3),\\ v &= V(T,r) + \varepsilon\tilde{v}(t,r,\theta) + \varepsilon^2\tilde{v}_2(t,r,\theta) + \mathcal{O}(\varepsilon^3),\\ h &= H(T,r) + \varepsilon\tilde{h}(t,r,\theta) + \varepsilon^2\tilde{h}_2(t,r,\theta) + \mathcal{O}(\varepsilon^3). \end{aligned}$$

The zeroth-order solution represents the vortex (which now depends on the slow time T), and the first-order solution represents a superposition of harmonic waves with various radial wavenumbers q and azimuthal wavenumbers k,

$$\tilde{u} = 2\mathrm{Re}\sum_{k=-\infty}^{\infty}\int_0^\infty a_k(q)\,\hat{u}e^{\mathrm{i}(k\theta-\omega t)}\mathrm{d}q, \tag{43}$$

$$\tilde{v} = 2\mathrm{Re}\sum_{k=-\infty}^{\infty}\int_0^\infty a_k(q)\,\hat{v}e^{\mathrm{i}(k\theta-\omega t)}\mathrm{d}q, \tag{44}$$

$$\tilde{h} = 2\mathrm{Re}\sum_{k=-\infty}^{\infty}\int_0^\infty a_k(q)\,\hat{h}e^{\mathrm{i}(k\theta-\omega t)}\mathrm{d}q. \tag{45}$$

In these expressions, $a_k(q)$ is the amplitude of an incident harmonic (q,k), and the functions $(\hat{u},\hat{v},\hat{h})$ satisfy the "old" boundary-value problem (19)–(22), (26) and (27), where the incident wave is of unit amplitude.

It should be emphasized that $a_k(q)$ is the amplitude of the incident wave far from the vortex, i.e., a characteristic of the background oceanic wave field. There are numerous measurements of its characteristics (e.g., Ref. 66 and the papers cited therein), but it is not clear how $a_k(q)$ can be inferred from those: mathematically, we need to "extract" from a random wave field the waves that converge on a given vortex. This issue is examined in Appendix D.

It is also argued in Appendix D that random waves with different wavenumbers are uncorrelated, which mathematically amounts to

$$\langle a_k(q)\, a_{k_1}(q_1)\rangle = 0, \tag{46}$$

$$\langle a_k(q)\, a^*_{k_1}(q_1)\rangle = A(q)\,\delta(q-q_1)\,\delta_{k,k_1}, \tag{47}$$

where the angled brackets denote ensemble averaging, $\delta(q-q_1)$ is the Dirac delta function, and δ_{k,k_1} is the Kronecker delta. The real, positive function $A(q)$ is a characteristic of the background wave field; as shown in Appendix D, it can be inferred from the two-point correlation function of the free-surface elevation (which is one of the most common characteristics measured in the ocean).

The vortex evolution is described by the averaged version of the second-order equations, of which only two are needed [(40) yields the second-order gradient-wind balance relating $\langle\tilde{v}_2\rangle$ to $\langle\tilde{h}_2\rangle$, neither of which happens to contribute to the vortex's dynamics]. We shall also replace the second-order version of the azimuthal equation (41) with that of the energy equation (9) (which shortens calculations and is helpful for physical interpretation). Finally note that the averaged solution is independent of the fast time t and azimuthal angle θ.

With all this in mind, one can write the averaged second-order versions of Eqs. (9) and (42) in the form

$$r\frac{\partial H}{\partial T} + \frac{\partial\left[r\left(\langle\tilde{u}\tilde{h}\rangle + \langle\tilde{u}_2\rangle H\right)\right]}{\partial r} = 0, \tag{48}$$

$$\begin{aligned} &r\frac{\partial}{\partial T}\left(H\frac{V^2}{2} + \frac{H^2}{2}\right) + \frac{\partial}{\partial r}\left\{r\left[\langle\tilde{u}_2\rangle\left(H\frac{V^2}{2} + H^2\right)\right.\right.\\ &\left.\left. + \langle\tilde{u}\tilde{v}\rangle HV + \langle\tilde{u}\tilde{h}\rangle\left(\frac{V^2}{2} + 2H\right)\right]\right\} = 0. \end{aligned} \tag{49}$$

Evidently, these equations include the Reynolds stress, $\langle\tilde{u}\tilde{h}\rangle$ and $\langle\tilde{u}\tilde{v}\rangle$: these can be calculated using expressions (43)–(45), simplified using Eqs. (46) and (47), and then $\hat{u}$ and $\hat{v}$ can be expressed through $\hat{h}$ via (19) and (20). Eventually, we obtain

$$\langle\tilde{u}\tilde{h}\rangle = \sum_{k=-\infty}^{\infty}\int_0^\infty A(q)\frac{\mathrm{i}F}{H}\left(\omega - \frac{kV}{r}\right)\left(\frac{\partial\hat{h}}{\partial r}\hat{h}^* - \frac{\partial\hat{h}^*}{\partial r}\hat{h}\right)\mathrm{d}q,$$

$$\langle\tilde{u}\tilde{v}\rangle = \sum_{k=-\infty}^{\infty}\int_0^\infty A(q)\frac{\mathrm{i}kF}{rH}\left(\frac{\partial\hat{h}}{\partial r}\hat{h}^* - \frac{\partial\hat{h}^*}{\partial r}\hat{h}\right)\mathrm{d}q.$$

Substituting these expressions into Eqs. (48) and (49) and replacing $\langle\tilde{u}_2\rangle$ with a new variable U defined by

$$\begin{aligned} U = rH\langle\tilde{u}_2\rangle &+ \sum_{k=-\infty}^{\infty}\int_0^\infty A(q)\frac{\mathrm{i}rF}{H}\left(\omega - \frac{kV}{r}\right)A^2\left(\frac{\partial\hat{h}}{\partial r}\hat{h}^* - \frac{\partial\hat{h}^*}{\partial r}\hat{h}\right)\mathrm{d}q, \end{aligned} \tag{50}$$

we obtain

$$r\frac{\partial H}{\partial T} + \frac{\partial U}{\partial r} = 0, \tag{51}$$

$$r\frac{\partial}{\partial T}\left(H\frac{V^2}{2}+\frac{H^2}{2}\right)+\frac{\partial}{\partial r}\left[\left(\frac{V^2}{2}+H\right)U\right]+\sum_{k=-\infty}^{\infty}\int_0^{\infty}\omega A(q)\frac{\partial}{\partial r}\left[irF\left(\frac{\partial\hat{h}}{\partial r}\hat{h}^*-\frac{\partial\hat{h}^*}{\partial r}\hat{h}\right)\right]dq=0. \quad (52)$$

These two equations govern the depth $H(T,r)$ and the radial mass flux $U(T,r)$. The swirl velocity $V(T,r)$ can be deduced from the leading-order gradient-wind balance (7). The function $\hat{h}$ (describing scattering of an incident wave of unit amplitude) is determined by the old boundary-value problem (22), (26) and (27). Finally, the function $A(q)$ describes the amplitudes of waves coming from infinity and, thus, should be viewed as a given coefficient.

Note also that the two terms in expression (50) for the mass flux U represent the flow generated by the wave–vortex interaction and the Stokes drift (a weak flow due to the wave's nonlinearity).

B. Discussion

To understand the physical meaning of the equations derived, note that the second and third terms in Eq. (52) represent the energy fluxes carried by the mean flow and the waves, respectively. Evidently, the latter flux involves the Wronskian (28), which is piece-wise constant and "jumps" only at the wave's critical levels, making these the only points where the wave–vortex energy exchange takes place.

Observe that Eq. (52) includes the derivative of the Wronskian, so that a jump of Wr gives rise to a delta function describing a point source or sink. The positions of these sources/sinks depend on the harmonic's wavenumbers q and k; hence, upon integration with respect to the former, the source term in Eq. (52) should become finite and continuous.

The only exception from this conclusion is a situation where hyper-reflection occurs.

To understand why, consider a ring (vortex with non-monotonic dependence of the angular velocity on r), in which case incident waves may have either one or two critical levels. As stated before, hyper-reflection typically occurs in the latter case; thus, let the radii of the two critical levels be r_1 and r_2. Denoting the corresponding Wronskian jumps by Δ_1 and Δ_2, we conclude that

$$\frac{\partial}{\partial r}\left[irF\left(\frac{\partial\hat{h}}{\partial r}\hat{h}^*-\frac{\partial\hat{h}^*}{\partial r}\hat{h}\right)\right]=\Delta_1\delta(r-r_1)+\Delta_2\delta(r-r_2),$$

whereas formulas (29) show that

$$\Delta_1+\Delta_2=\frac{2}{q}\left(|R|^2-1\right). \quad (53)$$

Note that, for an over-reflected wave, $\Delta_1+\Delta_2>0$.

Now, consider a hyper-reflected harmonic (q_h,k_h) and recall that, as established in Sec. III B 2,

$$|R|^2\sim|q-q_h|^{-2}\quad\text{as}\quad q\to q_c.$$

As a result, the integral with respect to q in the third term of the energy equation (52) diverges at $r=r_1$ and/or $r=r_2$. Common sense and the sign of the right-hand side or equality (53) indicate that the net energy flux carried away by the hyper-reflected wave is positive, suggesting that it drains a significant share of the vortex's energy in a short time.

It does not, however, drain all of the vortex's energy.

To understand why, recall that hyper-reflecting vortices do not represent the generic situation: for vortices (38), for example, they correspond to isolated curves in the (r_v,W) parameter plane. Thus, it is safe to assume that generic variations of the vortex's profile stop hyper-reflection, including a variation caused by the energy drain to an H-R wave. In other words, a hyper-reflecting vortex "tunes itself out" of hyper-reflection.

Another interesting scenario arises when an initially non-hyper-reflecting vortex becomes one while evolving under the influence of an external factor (e.g., bottom friction, slowing the flow down). A definitive answer as to what happens in this case can only be obtained via simulation of evolution equations (51) and (52), but, unfortunately, this is not an easy task: they are coupled to the scattering boundary-value problem (22), (26) and (27), which needs to be solved at each time step for each wave of the spectrum.

In contrast with vortices, the behavior of straight jets is clear: all of these hyper-reflect and, thus, cannot tune themselves out of hyper-reflection, hence, quickly lose energy. Only curved or zigzagging jets can avoid hyper-reflection, which is qualitatively consistent with observations, as most oceanic jets meander.

VI. CONCLUDING REMARKS

The main conclusion of this work is that hyper-reflection can occur for vortices, but only for ring-like ones, whose widths W are noticeably smaller than their radii r_v (it remains to be seen how often such vortices arise in the oceans and atmospheres of real planets). Small rings and eddies (with $W\sim r_v$) can over-reflect, but not hyper-reflect.

It has also been shown that hyper-reflection is always a sign of radiative instability, so that any change of the ring's parameters renders the hyper-reflected wave unstable. The converse does not hold, however: rings that are unstable at sub-inertial frequencies cannot radiate inertia-gravity waves, hence, cannot hyper-reflect.

It should be noted that the mostly numerical results presented in this paper can be complemented by analytical approaches, e.g., by examining the asymptotic limit of small Froude number (similar to Ref. 31), or by studying the WKB limit of waves (similar to Refs. 34 and 56), or by exploring the wave-flow energy exchange (similar to Refs. 56 and 57). The problems examined in these papers are similar to ours, and their results should be qualitatively relevant, or perhaps even applicable. Our understanding of wave–vortex interaction can also be advanced through the slow-evolution equations (51) and (52), possibly under the additional assumption that the waves are short, so that the WKB approximation applies.

Note that our conclusions do not apply to draining (bathtub) vortices, which over-reflect due to a turning point, not a critical level. One should still expect a certain degree of likeness between the two kinds of vortices. If indeed so, the shape of the drain and the bottom topography around it should alter the over-reflection coefficient and, potentially, can even turn it into hyper-reflection. As a result, bathtub vortices could over-reflect much stronger than the 14%±8% measured by Torres *et al.*[18]

It is worth commenting on whether hyper-reflection and related effects can be observed in an oceanic experiment: admittedly, the high costs of simultaneous measurements of a vortex and the wave field far from it make such an experiment difficult to perform. It should be much easier—and still informative—to carry out a numerical

experiment using a realistic ocean model, such as the Regional Ocean Modeling System[67] or the Nucleus for European Modeling of the Ocean.[68]

It would also be of interest to examine how H-R of waves by vortices is affected by nonlinear effects: given the high amplitude of the hyper-reflected wave, nonlinearity may be important. Similar studies for plane flows[69–71] suggest that, in the absence of viscosity, nonlinearity does not arrest hyper-reflection, potentially leading to the development of a finite-time singularity. If, however, viscosity is introduced into the model, one should expect it to regularize the singularity to a large but finite value, as well as—more generally—the entire effect of hyper-reflection.

ACKNOWLEDGMENTS

This work was supported in part by Taighde Éireann—Research Ireland under Grant 18/CRT/6049.

AUTHOR DECLARATIONS

Conflict of Interest

The authors have no conflicts to disclose.

Author Contributions

C. Nolan: Methodology (equal); Software (equal). **E. S. Benilov:** Conceptualization (equal); Formal analysis (equal); Methodology (equal); Project administration (equal); Writing – original draft (equal); Writing – review & editing (equal).

DATA AVAILABILITY

Data sharing is not applicable to this article as no new data were created or analyzed in this study.

APPENDIX A: BOUNDARY CONDITION AT THE CENTER OF THE VORTEX

The structure of the steady-state solution $\hat{h}(r)$ as $r \to 0$ cannot be clarified within the framework the steady-state equation (22), because the regular and the singular solutions differ by their physical meaning, not because one of them is mathematically incorrect.

In what follows, we show that the regular solutions are the ones emerging from the initial-value problem as $t \to \infty$. This conclusion is natural and intuitive, whereas the (forthcoming) derivation justifying it is cumbersome, yet the latter seems to provide the only means of ascertaining the former.

Observe that, as $r \to 0$, the swirl velocity $V(r)$ is close to zero, and the vortex thickness $H(r)$ is close to a constant (which can be scaled out of the problem). It is also reasonable to assume that the wave field near $r = 0$ does not depend on where the waves are coming from; hence, the wave source located at infinity can be replaced with one located at a finite r. These assumptions allow one to formulate a simple test problem clarifying the boundary condition at the center of the vortex in general.

Thus, let $V = 0$ and $H = 1$, and assume that waves with an azimuthal wavenumber k are generated by a circular, infinitely thin source located at $r = r_s$. In this case, Eqs. (10)–(12) become

$$\frac{\partial \tilde{u}}{\partial t} + \frac{\partial \tilde{h}}{\partial r} = \tilde{v}, \qquad \frac{\partial \tilde{v}}{\partial t} + \frac{1}{r}\frac{\partial \tilde{h}}{\partial \theta} = -\tilde{u}, \tag{A1}$$

$$r\frac{\partial \tilde{h}}{\partial t} + \frac{\partial (r\tilde{u})}{\partial r} + \frac{\partial \tilde{v}}{\partial \theta} = e^{\mathrm{i}(k\theta - \omega t)}\delta(r - r_s), \tag{A2}$$

where $\delta(r - r_s)$ is the Dirac delta. One could also insert source terms in Eqs. (A1) (which would correspond physically to a slightly different way of generating waves), but these would only make the algebra more tedious without changing the final conclusion.

Equations (A1) and (A2) will be solved with the simplest initial condition,

$$\hat{u} = 0, \qquad \hat{v} = 0, \qquad \hat{h} = 0 \quad \text{at} \quad t = 0. \tag{A3}$$

One can safely assume that a singularity at $r = 0$ cannot develop at a finite t; hence,

$$\hat{u} \to 0, \qquad \hat{v} \to 0, \qquad \hat{h} \to 0 \quad \text{as} \quad r \to 0. \tag{A4}$$

We emphasize that this boundary condition does not rule out a singularity emerging as $t \to \infty$.

It can be verified by inspection that the solution can be sought in the form

$$\tilde{u} = u'(t, r)e^{\mathrm{i}k\theta}, \qquad \tilde{v} = v'(t, r)e^{\mathrm{i}k\theta}, \qquad \tilde{h} = h'(t, r)e^{\mathrm{i}k\theta},$$

so that Eqs. (A1)–(A4) become

$$\frac{\partial u'}{\partial t} + \frac{\partial h'}{\partial r} = v', \qquad \frac{\partial v'}{\partial t} + \frac{\mathrm{i}kh'}{r} = -u',$$
$$r\frac{\partial h'}{\partial t} + \frac{\partial (ru')}{\partial r} + \mathrm{i}kv' = e^{-\mathrm{i}\omega t}\delta(r - r_s).$$

It can be verified by inspection

$$u' = 0, \qquad v' = 0, \qquad h' = 0 \quad \text{at} \quad t = 0,$$
$$u' \to 0, \qquad v' \to 0, \qquad h' \to 0 \quad \text{as} \quad r \to 0.$$

This initial-boundary-value problem can be solved using the Laplace transformation. Denoting the transforms using overbars, e.g.,

$$\bar{u}(s, r) = \int_0^\infty u'(t, r)e^{-st}\mathrm{d}t,$$

one can express $\bar{u}$ and $\bar{v}$ through $\bar{h}$ and thus show that $\bar{h}$ satisfies

$$\frac{1}{r}\frac{\partial}{\partial r}\left(r\frac{\partial \bar{h}}{\partial r}\right) - \left(s^2 + 1 + \frac{k^2}{r^2}\right)\bar{h} = -\frac{s^2 + 1}{s(s + \mathrm{i}\omega)r_s}\delta(r - r_s), \tag{A5}$$

$$\bar{h} \to 0 \quad \text{as} \quad r \to 0. \tag{A6}$$

Equation (A5) and boundary condition (A6) do not fully determine the solution, as one also needs a condition as $r \to \infty$. Since the source in our setting is at a finite r, waves are not coming from infinity – mathematically, this corresponds to

$$\bar{h} = C_\infty r^{-1/2}e^{\mathrm{i}qr} + \mathcal{O}(r^{-3/2}) \quad \text{as} \quad r \to \infty, \tag{A7}$$

where the constant C_∞ is to be fixed later, and

$$q = \sqrt{-s^2 - 1}, \tag{A8}$$

where the branch of the square root on the plane of complex s is fixed by a cut along the segment $(-\mathrm{i}, \mathrm{i})$ and the condition

$$\mathrm{Re}\, q > 0 \quad \text{if} \quad \mathrm{Re}\left(-s^2 - 1\right) > 0, \tag{A9}$$

which guarantees that Eq. (A7) describes waves traveling away from the origin.

Following the standard approach to linear differential equations with a delta-function on the right-hand side (see pp. 16–19 of Ref. 72), one can deduce that the solution of Eq. (A5) is continuous at $r = r_s$,

$$\lim_{r\to r_s+0} \bar{h} - \lim_{r\to r_s-0} \bar{h} = 0, \tag{A10}$$

while its derivative jumps by the amount equal to the coefficient of the delta function,

$$\lim_{r\to r_s+0} \frac{\partial \bar{h}}{\partial r} - \lim_{r\to r_s-0} \frac{\partial \bar{h}}{\partial r} = -\frac{s^2+1}{s(s+\mathrm{i}\omega) r_s}. \tag{A11}$$

The boundary-value problem comprising Eq. (A5), boundary conditions (A6) and (A7), and matching conditions (A10) and (A11) can be readily solved. We only need the solution for $r < r_s$, which is

$$\bar{h} = \frac{\mathrm{i}\pi(s^2+1)\left[J_{|k|}(qr_s) + \mathrm{i}Y_{|k|}(qr_s)\right]}{2s(s+\mathrm{i}\omega)} J_{|k|}(qr),$$

where J_k and Y_k are the Bessel functions of the first and second kind, respectively.

To find the original function $h'(t, r)$, one needs to calculate the inverse transform of $\bar{h}(s, r)$,

$$h' = \int_{\sigma-\mathrm{i}\infty}^{\sigma+\mathrm{i}\infty} \frac{\mathrm{i}(s^2+1)\left[J_{|k|}(qr_s) + \mathrm{i}Y_{|k|}(qr_s)\right]}{4s(s+\mathrm{i}\omega)} J_{|k|}(qr) e^{st}\,\mathrm{d}s,$$

where σ is a real positive number. The integrand in this integral is analytic except:

(1) the point $s = -\mathrm{i}\omega$ where it has a first-order pole,
(2) the cut $(-\mathrm{i}, \mathrm{i})$ across which it has a jump [caused by that of q—see Eqs. (A8) and (A9)].

Thus, one can reduce the above expression to

$$h' = -\frac{\pi(\omega^2-1)\left[J_{|k|}\left(\sqrt{\omega^2-1}r_s\right) + \mathrm{i}Y_{|k|}\left(\sqrt{\omega^2-1}r_s\right)\right]}{2\mathrm{i}\omega} J_{|k|}\left(\sqrt{\omega^2-1}r\right) \times e^{-\mathrm{i}\omega t} + \oint \frac{\mathrm{i}(s^2+1)\left[J_{|k|}(qr_s) + \mathrm{i}Y_{|k|}(qr_s)\right]}{4s(s+\mathrm{i}\omega)} J_{|k|}(qr) e^{st}\,\mathrm{d}s, \tag{A12}$$

where the integral is to be evaluated around the cut $(-\mathrm{i}, \mathrm{i})$ counterclockwise.

The first term in expression (A12) describes a steady wave field of frequency ω; its spatial structure is determined by $J_{|k|}\left(\sqrt{\omega^2-1}r\right)$, which is regular as $r \to 0$ and satisfies boundary condition (27). The second term is also regular, but is irrelevant to the steady problem: it describes a continuous spectrum of "quasimodes," i.e., interfering (cancelling each other) waves, decaying as $t \to \infty$ (as continuous-spectrum disturbances do in parallel flows[48,49] and vortices[73]).

APPENDIX B: ASYMPTOTICS OF THE SOLUTION NEAR APPARENT SINGULARITIES

Near an apparent singularity, expression (21) yields

$$F = \frac{F_{-1}}{\xi - \beta_a \mathrm{i}0} + F_0 + \mathcal{O}(\xi) \quad \text{as} \quad \xi \to 0, \tag{B1}$$

where $\xi = r - r_a$,

$$\beta_a = \mathrm{sign}\left[F_{-1}\left(\omega - \frac{kV}{r}\right)_{r=r_a}\right], \tag{B2}$$

and the expressions for F_{-1} and F_0 will not be needed. Given Eqs. (B1) and (B2) and equality (31), one can deduce the following limiting form of Eq. (22):

$$\frac{\mathrm{d}}{\mathrm{d}\xi}\left\{\left[\frac{r_a}{\xi - \beta_a \mathrm{i}0} + 1 + \frac{r_a F_0}{F_{-1}} + \mathcal{O}(\xi)\right]\frac{\mathrm{d}h}{\mathrm{d}\xi}\right\} + \left[\frac{r_a A}{(\xi - \beta_a \mathrm{i}0)^2} + \mathcal{O}(1)\right] h = 0 \quad \text{as} \quad \xi \to 0, \tag{B3}$$

where

$$A = \frac{k\left(1 + \frac{2V_a}{r_a}\right)}{r_a\left(\omega - \frac{kV_a}{r_a}\right)},$$

and $V_a = V(r_a)$. Equation (B3) admits two linearly independent solutions,

$$\hat{h}_1 = \xi^2 + \mathcal{O}(\xi^3), \qquad \hat{h}_2 = 1 + A\xi + \mathcal{O}(\xi^3 \ln \xi) \quad \text{as} \quad \xi \to 0. \tag{B4}$$

Then, expression (28) with $\hat{h}$ represented by an arbitrary linear combination of $\hat{h}_1$ and $\hat{h}_2$ shows that the Wronskian is continuous at r_a.

We have also calculated the term $\mathcal{O}(\xi^3 \ln \xi)$ in expansion (B4), and it turned out to be zero. This cancelation suggests that apparent singularities can be completely removed from Eq. (22) by a suitable substitution, the same way this was done by Vanneste and Yavneh[56] for a straight flow with constant shear on the f-plane. Our setting is slightly different, however: a curved flow and variable shear. As a result, it is not evident that the substitution suggested by Vanneste and Yavneh[56] eliminates all of the singular terms in our Eq. (22).

Numerically, the apparent singularities can be handled in the same way as critical levels, so the absence of a rigorous proof of regularity of $\hat{h}$ at $r = r_a$ does not pose a problem.

APPENDIX C: COMPUTATION OF THE REFLECTION COEFFICIENT

When computing the reflection coefficient R numerically, one has to handle the singular points of Eq. (22): the origin $r = 0$, the infinity $r \to \infty$, the critical levels (there can be either one or two of these), and the apparent singularities (also one or two).

To avoid the singularity at the origin, the left end point of the integration path was moved to $r = r_0$ ($0 < r_0 \ll 1$), and the boundary condition there was set according to asymptotics (27),

$$\hat{h} = Cr_0^{|k|}, \quad \frac{\mathrm{d}\hat{h}}{\mathrm{d}r} = C|k|r_0^{|k|-1} \quad \text{at} \quad r = r_0, \tag{C1}$$

where C is an undetermined constant. The singularity at infinity was "moved" to a finite point $r = r_\infty$ ($1 \ll r_\infty < \infty$), and the boundary condition there was set according to asymptotics (26),

$$\hat{h} = r_\infty^{-1/2}(e^{-\mathrm{i}qr_\infty} + Re^{\mathrm{i}qr_\infty}) \quad \frac{\mathrm{d}\hat{h}}{\mathrm{d}r} = \mathrm{i}qr_\infty^{-1/2}(-e^{-\mathrm{i}qr_\infty} + Re^{\mathrm{i}qr_\infty}) \quad \text{at} \quad r = r_\infty, \tag{C2}$$

Note that, in the condition for $\mathrm{d}\hat{h}/\mathrm{d}r$, the term $\sim r_\infty^{-3/2}$ was omitted because it is comparable to the error of the original asymptotics (26).

The parameters r_0 and r_∞ were chosen to ensure that, if they are doubled or halved, the computed reflection coefficient would not change by more than 10^{-5}. In practice, this requirement amounted to

$$10^{-3} \lesssim r_0 \lesssim 10^{-2},$$
$$r_v + 10^3 W \lesssim r_\infty \lesssim r_v + 10^4 r_v,$$

where r_v is the vortex's radius and W its width.

The problem's singularities were handled using the approach proposed by Boyd:[74] r was treated as a complex variable, and the path of integration was deformed to circumvent the critical levels. The semi-plane through which a particular critical level was circumvented was chosen in accordance with the sign of the parameter β_c given by Eq. (33): the critical level that is infinitesimally shifted upwards ($\beta_c > 0$) was circumvented through the lower semi-plane, and vice versa (see Fig. 7).

One of the apparent singularities is typically located between the critical levels, so that it can be avoided by adjusting the point where the path of integration crosses the real axis. The other apparent singularity is avoided automatically as the path of integration does not come back to the real axis until r_∞.

Observe that both boundary conditions involve unknown constants: conditions (C1) involve C, and condition (C2) involve R. This implies that the boundary-value problem (22), Eqs. (C1) and (C2) is to be solved iteratively.

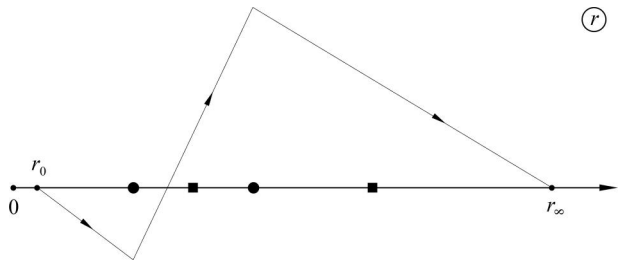

FIG. 7. Path of integration for Eq. (25) on the plane of complex r (a schematic). The circles and squares show the positions of the critical levels and apparent singularities, respectively.

A simpler approach—without iterations—consists in replacing $\hat{h}$ with

$$\hat{h}_{new} = \frac{\hat{h}}{C}.$$

As a result, the unknown parameter C is scaled out from conditions (C1), and the solution can be simply "shot" from $r = r_0$ toward $r = r_\infty$. Then, the reflection coefficient can be calculated using the solution computed at r_∞ via the formula

$$R = e^{-2\mathrm{i}qr_\infty}\frac{1-Q}{1+Q}$$

where

$$Q = \frac{\mathrm{i}}{q\hat{h}_{new}}\frac{\mathrm{d}\hat{h}_{new}}{\mathrm{d}r}.$$

Note that the described procedure yields the reflection coefficient R, but the eigenfunction $\hat{h}$ is computed for complex values of the coordinate r. To find $\hat{h}(r)$ for real r, one needs to compute the solution numerically on the real axis between the singular points of Eq. (22), then patch the piece-wise solution using asymptotic expansions about the singular points. For sufficient accuracy, 3–4 terms must be calculated analytically in each expansion, making this approach cumbersome and time-consuming.

If, however, $\mathrm{Im}\,\omega \neq 0$, Eq. (22) does not have singular points on the real axis, and the above difficulty does not arise. This is how unstable solutions graphed in Fig. 6 were computed.

Finally, once the integration path was specified, the solution was computed along it using the explicit (4,5) Runge–Kutta formula,[75] as implemented in MATLAB's ODE45 function.

APPENDIX D: DERIVATION OF CONDITIONS (46) AND (47)

This paper employs a cylindrical representation of waves, whereas real wave spectra are typically measured in Cartesian form. Thus, we need to be able to subdivide a Cartesian spectrum into cylindrical waves traveling toward a given vortex and those traveling away from it. The former are, essentially, incident waves [and, thus, should satisfy conditions (46) and (47)], whereas the latter are unimportant, as they simply merge with the wave field reflected by the vortex.

In what follows, we first derive the Cartesian versions of conditions (46) and (47), then convert them to the cylindrical form, as required.

1. The Cartesian equivalent of conditions (46) and (47)

Introduce the horizontal Cartesian coordinates $\mathbf{r} = (x, y)$, so that the elevation of the free surface generated by a spectrum of random waves is given by

$$\tilde{h}(\mathbf{r}, t) = 2\mathrm{Re}\int \eta(\mathbf{q})e^{\mathrm{i}(\mathbf{q}\cdot\mathbf{r}-\omega t)}\mathrm{d}^2\mathbf{q}, \tag{D1}$$

where $\eta(\mathbf{q})$ is the amplitude of a harmonic $\mathbf{q} = (q_x, q_y)$, and $\omega = (1 + q_x^2 + q_y^2)^{1/2}$ is its frequency. We define the two-point correlation function by

$$C(\mathbf{r}_1, \mathbf{r}_2) = \langle \tilde{h}(\mathbf{r}_1)\, \tilde{h}(\mathbf{r}_2) \rangle, \tag{D2}$$

where $\langle \cdots \rangle$ denotes the average of $\cdots$. Substituting (D1) into (D2), one obtains

$$C(\mathbf{r}_1, \mathbf{r}_2) = 2\mathrm{Re} \int\int \Big\{ \langle \eta(\mathbf{q}_1)\, \eta(\mathbf{q}_2) \rangle e^{\mathrm{i}[\mathbf{q}_1 \cdot \mathbf{r}_1 + \mathbf{q}_2 \cdot \mathbf{r}_2 - (\omega + \omega_2)t]} + \langle \eta(\mathbf{q}_1)\, \eta^*(\mathbf{q}_2) \rangle e^{-\mathrm{i}[\mathbf{q}_1 \cdot \mathbf{r}_1 - \mathbf{q}_2 \cdot \mathbf{r}_2 - (\omega - \omega_2)t]} \Big\} \mathrm{d}^2\mathbf{q}_1 \mathrm{d}^2\mathbf{q}_2. \tag{D3}$$

Let the wave field be spatially homogeneous, so that C depends only on $\mathbf{r}_1 - \mathbf{r}_2$ (not on $\mathbf{r}_1$ and $\mathbf{r}_2$ separately). Then it follows from (D3) that

$$\langle \eta(\mathbf{q}_1)\, \eta(\mathbf{q}_2) \rangle = 0, \tag{D4}$$

$$\langle \eta(\mathbf{q}_1)\, \eta^*(\mathbf{q}_2) \rangle = A(\mathbf{q}_1)\, \delta(\mathbf{q}_1 - \mathbf{q}_2), \tag{D5}$$

where the latter equality implies that $A_{\mathbf{q}_1} \geq 0$. Equalities (D4)–(D5) are standard parts of the theory of random waves originating from the seminal paper by Hasselmann.[76]

Assume additionally that the wave field is isotropic, so that $C(\mathbf{r})$ depends only on $r = |\mathbf{r}|$ and $A(\mathbf{q})$ depends only on $q = |\mathbf{q}|$. Now, substituting (D4)–(D5) into (D3) and letting $\mathbf{r}_1 - \mathbf{r}_2 = \mathbf{r}$, one obtains

$$C(r) = \int A(q) \cos(\mathbf{q} \cdot \mathbf{r})\, \mathrm{d}^2\mathbf{q}. \tag{D6}$$

Note that, if the correlation function $C(r)$ is known, one can readily deduce $A(q)$ from (D6) via the inverse Fourier transformation.

2. Cartesian and cylindrical wave spectra

Consider a vortex located at the origin, $\mathbf{r} = \mathbf{0}$, and introduce the polar coordinates in both (x, y) and (q_x, q_y) planes,

$$x = r\cos\theta, \quad y = r\sin\theta,$$
$$q_x = q\cos\phi, \quad q_y = q\sin\phi.$$

Then, expression (D1) for the wave field becomes

$$\tilde{h} = 2\mathrm{Re} \int_0^{2\pi} \int_0^{\infty} \eta(q, \phi) e^{\mathrm{i}[qr\cos(\theta - \phi) - \omega_q t]}\, q\, \mathrm{d}q\, \mathrm{d}\phi.$$

Next, expand $\tilde{h}$ in a Fourier series with respect to θ,

$$\tilde{h}(r, \theta) = \sum_{k=-\infty}^{\infty} \tilde{h}_k(q, r, t)\, e^{\mathrm{i}k\theta}, \tag{D7}$$

where the Fourier coefficients are

$$\tilde{h}_k(q, r, t) = \frac{1}{2\pi} \int_0^{2\pi} \left\{ 2\mathrm{Re} \int_0^{2\pi} \int_0^{\infty} \eta(q, \phi) e^{\mathrm{i}[qr\cos(\theta - \phi) - \omega_q t]} q\, \mathrm{d}q\, \mathrm{d}\phi \right\} e^{-\mathrm{i}k\theta}\, \mathrm{d}\theta. \tag{D8}$$

To extract from this expression the boundary condition for the scattering problem, one needs the asymptotics of Eq. (D8) as $r \to \infty$. Applying, thus, the stationary phase method and substituting the resulting expression for $\tilde{h}_k(q, r, t)$ into Eq. (D7), one obtains after straightforward algebra,

$$\tilde{h} = 2\mathrm{Re} \int_0^{\infty} \sum_{k=-\infty}^{\infty} \left[a_k(q) \frac{e^{\mathrm{i}(qr + k\theta - \omega_q t)}}{\sqrt{r}} + a_k(q) e^{-\mathrm{i}\pi\left(k - \frac{1}{2}\right)} \frac{e^{\mathrm{i}(-qr + k\theta - \omega_q t)}}{\sqrt{r}} \right] \mathrm{d}q, \tag{D9}$$

where

$$a_k(q) = \frac{\sqrt{q} e^{-\mathrm{i}\pi/4}}{\sqrt{2\pi}} \int_0^{2\pi} \eta(q, \phi) e^{-\mathrm{i}k\phi}\, \mathrm{d}\phi. \tag{D10}$$

The first and second terms in the square brackets (D9) represent the waves traveling toward and away from the vortex, respectively, and expression (D10) for $a_k(q)$ provides the amplitude of the former (it is the same as $a_k(q)$ in Eq. (45) of the main body of the paper).

Calculating $\langle a_k(q)\, a_k(q) \rangle$ and $\langle a_k(q)\, a_k^*(q) \rangle$, recalling the Cartesian conditions (D4) and (D5), assuming isotropy [so that $A(q, \phi)$ depends only on q], and keeping in mind that, in polar coordinates,

$$\delta(\mathbf{q}_1 - \mathbf{q}_2) = \frac{1}{q_1} \delta(q_1 - q_2)\, \delta(\phi_1 - \phi_2),$$

we obtain conditions (46) and (47) as required.

REFERENCES

[1] W. L. Jones, "Reflexion and stability of waves in stably stratified fluids with shear flow: A numerical study," J. Fluid Mech. **34**, 609–624 (1968).
[2] R. E. Dickinson, "Development of a Rossby wave critical level," J. Atmos. Sci. **27**, 627–633 (1970).
[3] J. F. McKenzie, "Reflection and amplification of acoustic-gravity waves at a density and velocity discontinuity," J. Geophys. Res. **77**, 2915–2926, https://doi.org/10.1029/JA077i016p02915 (1972).
[4] R. S. Lindzen, "Stability of a Helmholtz velocity profile in a continuously stratified, infinite Boussinesq fluid—Applications to clear air turbulence," J. Atmos. Sci. **31**, 1507–1514 (1974).
[5] I. A. Eltayeb and J. F. McKenzie, "Critical-level behaviour and wave amplification of a gravity wave incident upon a shear layer," J. Fluid Mech. **72**, 661–671 (1975).
[6] D. J. Acheson, "On over-reflexion," J. Fluid Mech. **77**, 433–472 (1976).
[7] C. A. van Duin and H. Kelder, "Reflection properties of internal gravity waves incident upon a hyperbolic tangent shear layer," J. Fluid Mech. **120**, 505–521 (1982).
[8] A. Y. Basovich and L. S. Tsimring, "Internal waves in a horizontally inhomogeneous flow," J. Fluid Mech. **142**, 233–249 (1984).
[9] S.-I. Takehiro and Y.-Y. Hayashi, "Over-reflection and shear instability in a shallow-water model," J. Fluid Mech. **236**, 259–279 (1992).
[10] M. C. Öllers, L. P. J. Kamp, F. Lott, P. F. J. van Velthoven, H. M. Kelder, and F. W. Sluijter, "Propagation properties of inertia–gravity waves through a barotropic shear layer and application to the Antarctic polar vortex," Q. J. R. Meteorol. Soc. **129**, 2495–2511 (2003).
[11] D. Gogichaishvili, G. Chagelishvili, R. Chanishvili, and J. Lominadze, "Nature and dynamics of overreflection of Alfvén waves in MHD shear flows," J. Plasma Phys. **80**, 667–685 (2014).
[12] S. Kim and K. Kim, "Giant overreflection of magnetohydrodynamic waves from inhomogeneous plasmas with nonuniform shear flows," Phys. Fluids **34**, 127108 (2022).
[13] Y. Zhang, S. Görtz, and M. Oberlack, "Over-reflection of acoustic waves by supersonic exponential boundary layer flows," J. Fluid Mech. **945**, A9 (2022).
[14] C. T. Rhodes, V. Limpasuvan, and Y. Orsolini, "The composite response of traveling planetary waves in the middle atmosphere surrounding sudden

stratospheric warmings through an overreflection perspective," J. Atmos. Sci. **80**, 2635–2652 (2023).
[15]G. M. Golemshtok and A. L. Fabrikant, "Scattering and amplification of sound waves by cylindrical vortex," Akust. Zh. **26**, 383–390 (1980).
[16]V. F. Kop'ev and E. A. Leont'ev, "Radiation and scattering of sound from a vortex ring," Fluid Dyn. **22**, 398–409 (1987).
[17]M. Richartz, A. Prain, S. Liberati, and S. Weinfurtner, "Rotating black holes in a draining bathtub: Superradiant scattering of gravity waves," Phys. Rev. D **91**, 124018 (2015).
[18]T. Torres, S. Patrick, A. Coutant, M. Richartz, E. W. Tedford, and S. Weinfurtner, "Rotational superradiant scattering in a vortex flow," Nat. Phys. **13**, 833–836 (2017).
[19]S. Churilov and Y. Stepanyants, "Scattering of surface shallow water waves on a draining bathtub vortex," Phys. Rev. Fluids **4**, 034704 (2019).
[20]R. Brito, V. Cardoso, and P. Pani, *Superradiance: New Frontiers in Black Hole Physics*, Lecture Notes in Physics No. 971 (Springer, Heidelberg, 2020).
[21]A. E. Gill, "Instabilities of "top-hat" jets and wakes in compressible fluids," Phys. Fluids **8**, 1428–1430 (1965).
[22]W. Blumen, P. G. Drazin, and D. F. Billings, "Shear layer instability of an inviscid compressible fluid. Part 2," J. Fluid Mech. **71**, 305–316 (1975).
[23]D. P. Lalas and F. Einaudi, "On the characteristics of gravity waves generated by atmospheric shear layers," J. Atmos. Sci. **33**, 1248–1259 (1976).
[24]R. S. Lindzen and A. J. Rosenthal, "On the instability of Helmholtz velocity profiles in stably stratified fluids when a lower boundary is present," J. Geophys. Res. **81**, 1561–1571, https://doi.org/10.1029/JC081i009p01561 (1976).
[25]R. S. Lindzen and K. K. Tung, "Wave overreflection and shear instability," J. Atmos. Sci. **35**, 1626–1632 (1978).
[26]E. G. Broadbent and D. W. Moore, "Acoustic destablilization of vortices," Philos. Trans. R. Soc. London **290**, 353–371 (1979).
[27]P. A. Davis and W. R. Peltier, "Some characteristics of the Kelvin-Helmholtz and overreflection modes of shear flow and of their interaction through vortex pairing," J. Atmos. Sci. **36**, 2394–2412 (1979).
[28]A. J. Rosenthal and R. S. Lindzen, "Instabilities in a stratified fluid having one critical level. Part II: Explanation of gravity wave instabilities using the concept of overreflection," J. Atmos. Sci. **40**, 521–529 (1983).
[29]R. S. Lindzen and J. W. Barker, "Instability and wave over-reflection in stably stratified shear flow," J. Fluid Mech. **151**, 189 (1985).
[30]R. S. Lindzen, "Instability of plane parallel shear flow (toward a mechanistic picture of how it works)," Pure Appl. Geophys. **126**, 103–121 (1988).
[31]F. Ford, "The instability of an axisymmetric vortex with monotonic potential vorticity in rotating shallow water," J. Fluid Mech. **280**, 303–334 (1994).
[32]N. J. Balmforth, "Shear instability in shallow water," J. Fluid Mech. **387**, 97–127 (1999).
[33]R. Ford, M. E. McIntyre, and W. A. Norton, "Balance and the slow quasimanifold: Some explicit results," J. Atmos. Sci. **57**, 1236–1254 (2000).
[34]S. Le Dizès and P. Billant, "Radiative instability in stratified vortices," Phys. Fluids **21**, 096602 (2009).
[35]X. Riedinger and A. Gilbert, "Critical layer and radiative instabilities in shallow-water shear flows," J. Fluid Mech. **751**, 539–569 (2014).
[36]T. S. Eaves and N. J. Balmforth, "Instability of sheared density interfaces," J. Fluid Mech. **860**, 145–171 (2019).
[37]C. Wang, A. Gilbert, and J. Mason, "Critical-layer instability of shallow-water magnetohydrodynamic shear flows," J. Fluid Mech. **943**, A24 (2022).
[38]M. E. McIntyre and M. A. Weissman, "On radiating instabilities and resonant overreflection," J. Atmos. Sci. **35**, 1190–1196 (1978).
[39]S. A. Maslowe, "Barotropic instability of the Bickley jet," J. Fluid Mech. **229**, 417–426 (1991).
[40]F. Lott, H. Kelder, and H. Teitelbaum, "A transition from Kelvin–Helmholtz instabilities to propagating wave instabilities," Phys. Fluids A **4**, 1990–1997 (1992).
[41]E. S. Benilov and V. N. Lapin, "On resonant over-reflection of waves by jets," Geophys. Astrophys. Fluid Dyn. **107**, 304–327 (2013).
[42]A. Viúdez and D. G. Dritschel, "Spontaneous generation of inertia–gravity wave packets by balanced geophysical flows," J. Fluid Mech. **553**, 107 (2006).
[43]J. Pedlosky, *Geophysical Fluid Dynamics*, 2nd ed. (Springer, 1987).
[44]B. Cushman-Roisin and J.-M. Beckers, *Introduction to Geophysical Fluid Dynamics*, 2nd ed. (Academic Press, Amsterdam, 2011).
[45]N. Paldor and D. Nof, "Linear instability of an anticyclonic vortex in a two-layer ocean," J. Geophys. Res. **95**, 18075–18079, https://doi.org/10.1029/JC095iC10p18075 (1990).
[46]P. D. Killworth, J. R. Blundell, and W. K. Dewar, "Primitive equation instability of wide oceanic rings. Part 1: Linear theory," J. Phys. Oceanogr. **27**, 941–962 (1997).
[47]E. S. Benilov, "The effect of ageostrophy on the stability of thin oceanic vortices," Dyn. Atmos. Oceans **39**, 211–226 (2005).
[48]K. M. Case, "Stability of inviscid plane Couette flow," Phys. Fluids **3**, 143 (1960).
[49]L. A. Dikiy, "Stability of plane-parallel flows in an ideal fluid (in Russian)," Doklady AN SSSR **125**, 1068–1071 (1960).
[50]J. R. Booker and F. P. Bretherton, "The critical layer for internal gravity waves in a shear flow," J. Fluid Mech. **27**, 513–539 (1967).
[51]K. Stewartson, "The evolution of the critical layer of a Rossby wave," Geophys. Astrophys. Fluid Dyn. **9**, 185–200 (1977).
[52]D. J. Benney and R. F. Bergeron, "A new class of nonlinear waves in parallel flows," Stud. Appl. Math. **48**, 181–204 (1969).
[53]R. Haberman, "Critical layers m parallel flows," Stud. Appl. Math. **51**, 139–161 (1972).
[54]C. C. Lin, "On the stability of two-dimensional parallel flows. I. General theory," Q. Appl. Math. **3**, 117–142 (1945).
[55]J. P. Boyd, "Planetary waves and the semiannual wind oscillation in the tropical lower stratosphere," Ph.D. thesis (University of Harward, 1976).
[56]J. Vanneste and I. Yavneh, "Unbalanced instabilities of rapidly rotating stratified shear flows," J. Fluid Mech. **584**, 373–396 (2007).
[57]C. Wang and N. J. Balmforth, "Strato-rotational instability without resonance," J. Fluid Mech. **846**, 815–833 (2018).
[58]E. S. Benilov, D. Broutman, and E. P. Kuznetsova, "On the stability of large-amplitude vortices in a continuously stratified fluid on the *f*-plane," J. Fluid Mech. **355**, 139–162 (1998).
[59]E. S. Benilov, "Instability of quasi-geostrophic vortices in a two-layer ocean with a thin upper layer," J. Fluid Mech. **475**, 303–331 (2003).
[60]C. A. Katsman, P. C. F. van der Vaart, H. A. Dijkstra, and W. P. M. de Ruijter, "Stability of multi-layer ocean vortices: A parameter study including realistic Gulf Stream and Agulhas rings," J. Phys. Oceanogr. **33**, 1197–1218 (2003).
[61]E. S. Benilov and J. D. Flanagan, "The effect of ageostrophy on the stability of vortices in a two-layer ocean," Ocean Modell. **23**, 49–58 (2008).
[62]N. Paldor and M. Ghil, "Linear instability of a zonal jet on an *f*-plane," J. Phys. Oceanogr **27**, 2361–2369 (1997).
[63]F. J. Poulin and G. R. Flierl, "The nonlinear evolution of barotropically unstable jets," J. Phys. Oceanogr. **33**, 2173–2192 (2003).
[64]M. Müller, B. K. Arbic, J. G. Richman, J. F. Shriver, E. L. Kunze, R. B. Scott, A. J. Wallcraft, and L. Zamudio, "Toward an internal gravity wave spectrum in global ocean models," Geophys. Res. Lett. **42**, 3474–3481, https://doi.org/10.1002/2015GL063365 (2015).
[65]E. S. Benilov, V. G. Gnevyshev, and V. I. Shrira, "Nonlinear interaction of a zonal jet and barotropic Rossby-wave turbulence: The problem of turbulent friction," Dyn. Atmos. Oceans **16**, 339–353 (1992).
[66]S. M. Soares, S. T. Gille, T. K. Chereskin, and M. Passaro, "The sea surface height spectrum of internal waves," J. Geophys. Res. Oceans **130**, e2025JC023104, https://doi.org/10.1029/2025JC023104 (2025).
[67]A. F. Shchepetkin and J. C. McWilliams, "The regional oceanic modeling system (ROMS): A split-explicit, free-surface, topography-following-coordinate oceanic model," Ocean Modell. **9**, 347–404 (2005).
[68]P. Mathiot, A. Jenkins, C. Harris, and G. Madec, "Explicit representation and parametrised impacts of under ice shelf seas in the z^* coordinate ocean model NEMO 3.6," Geosci. Model Dev. **10**, 2849–2874 (2017).
[69]R. H. J. Grimshaw, "Nonlinear aspects of an internal gravity wave co-existing with an unstable mode associated with a Helmholtz velocity profile," J. Fluid Mech. **76**, 65–84 (1976).
[70]R. H. J. Grimshaw, "On resonant over-reflexion of internal gravity waves from a Helmholtz velocity profile," J. Fluid Mech. **90**, 161–178 (1979).

[71]R. H. J. Grimshaw, "Resonant over-reflection of internal gravity waves from a thin shear layer," J. Fluid Mech. **109**, 349–365 (1981).
[72]C. M. Bender and S. A. Orszag, *Advanced Mathematical Methods for Scientists and Engineers I* (Springer, New York, 1999).
[73]D. A. Schecter, D. H. E. Dubin, A. C. Cass, C. F. Driscoll, I. M. Lansky, and T. M. O'Neil, "Inviscid damping of asymmetries on a two-dimensional vortex," Phys. Fluids **12**, 2397–2412 (2000).
[74]J. P. Boyd, "Complex coordinate methods for hydrodynamic instabilities and Sturm-Liouville eigenproblems with an interior singularity," J. Comput. Phys. **57**, 454–471 (1985).
[75]J. R. Dormand and P. J. Prince, "A family of embedded Runge-Kutta formulae," J. Comput. Appl. Math. **6**, 19–26 (1980).
[76]K. Hasselmann, "On the non-linear energy transfer in a gravity-wave spectrum Part 1. General theory," J. Fluid Mech. **12**, 481–500 (1962).